ECOLOGY

Marine heatwaves threaten cryptic coral diversity and erode associations among coevolving partner

Samuel Starko[1,2]*, James E. Fifer[3], Danielle C. Claar[1,4], Sarah W. Davies[3], Ross Cunning[5], Andrew C. Baker[6], Julia K. Baum[1,7]*

Climate change–amplified marine heatwaves can drive extensive mortality in foundation species. However, a paucity of longitudinal genomic datasets has impeded understanding of how these rapid selection events alter cryptic genetic structure. Heatwave impacts may be exacerbated in species that engage in obligate symbioses, where the genetics of multiple coevolving taxa may be affected. Here, we tracked the symbiotic associations of reef-building corals for 6 years through a prolonged heatwave, including known survivorship for 79 of 315 colonies. Coral genetics strongly predicted survival of the ubiquitous coral, *Porites* (massive growth form), with variable survival (15 to 61%) across three morphologically indistinguishable—but genetically distinct—lineages. The heatwave also disrupted strong associations between these coral lineages and their algal symbionts (family Symbiodiniaceae), with symbiotic turnover in some colonies, resulting in reduced specificity across lineages. These results highlight how heatwaves can threaten cryptic genotypes and decouple otherwise tightly coevolved relationships between hosts and symbionts.

INTRODUCTION

Extreme climatic events, such as heatwaves, wildfires, floods, and droughts, have become substantial catalysts for ecological change, jeopardizing biodiversity and natural ecosystems worldwide (*1–3*). Such events are driving factors behind many species range contractions, extirpations, and invasions (*4–8*) and may also influence the genetic makeup of taxa through selection imposed by rapid environmental change (*9–11*). Recent studies have demonstrated that selection through extreme events can be directional, favoring individual genotypes or lineages that carry adaptive traits (*10, 12–14*). While this selection may drive adaptation and help taxa persist through similar types of future events, reductions in the diversity of genotypes or lineages may limit the capacity for future adaptation to disturbances of a different nature (*15, 16*), such as unexpected stressors and pathogens (*17*).

In the ocean, some of the most profound impacts of climate change are experienced during marine heatwaves (*5, 18*)—pulse heat stress events in which water temperatures are abnormally high for unusual lengths of time (*19, 20*). While it is established that heatwaves can threaten marine biodiversity by driving conspicuous species losses (*4, 5, 21*), selection imposed during heatwaves may also drive cryptic losses of diversity within taxa, such as the loss of morphologically indistinguishable genotypes or cryptic species that remain challenging to characterize (*9, 10, 12*). This phenomenon is predicted to be an outcome of extreme climatic events but, due to the lack of baseline genetic data, has only rarely been demonstrated in marine systems (*10, 12, 22, 23*). Losses of cryptic diversity could have long-term evolutionary consequences for taxa by limiting their scope for future adaptation (*10, 12, 24*). For example, introgression between differentiated lineages or cryptic species can be a critical mechanism behind rapid adaptation (*25, 26*), a process that would be hindered by the loss of cryptic diversity. Our ability to anticipate the true consequences of marine heatwaves will therefore depend on understanding the extent to which marine heatwaves drive differential mortality among cryptic genotypes, lineages, or species, thereby altering the genetic makeup of taxa (*10*). To date, the few studies that have investigated this phenomenon have demonstrated that marine heatwaves can alter the relative abundance of genotypes (*12, 22*), but linking these patterns to fitness components, which requires tracking survival and/or reproductive output of individuals, remains a challenge [but see (*23*)].

Under climate change, tropical reef-building corals may be particularly susceptible to losses of cryptic diversity, both because cryptic species complexes are exceptionally common in this group [e.g., (*27–30*)] and because corals are highly sensitive to thermal stress (*18*). Heatwaves disrupt the critical relationship between reef-building corals and their obligate endosymbionts (family Symbiodiniaceae), causing them to bleach (*18, 31, 32*) and making them vulnerable to starvation and disease (*33*). Intense or prolonged marine heatwaves can cause mass bleaching and widespread coral mortality, with profound ecological and socioeconomic impacts (*18*). This is especially true given that these ecosystems are the most biologically diverse and among the most economically valuable in the ocean (*34*). As in a wide range of taxa, molecular investigations of reef-building corals over the past two or more decades have drastically reshaped our understanding of their evolution and diversity [e.g., (*27, 32, 35*)]. Similar to macroalgae and other invertebrates [e.g., (*36, 37*)], many morphologically defined coral species actually represent cryptic species complexes consisting of multiple morphologically similar, or even indistinguishable, lineages that are partially or completely reproductively isolated from one another [e.g., (*27–30*)]. Moreover, constituent cryptic species or lineages

[1]Department of Biology, University of Victoria, PO Box 1700 Station CSC, Victoria, British Columbia V8W 2Y2, Canada. [2]UWA Oceans Institute and School of Biological Sciences, University of Western Australia, Crawley, WA 6009, Australia. [3]Department of Biology, Boston University, Boston, MA 02215, USA. [4]Washington Department of Natural Resources, Olympia, WA 98504, USA. [5]Daniel P. Haerther Center for Conservation and Research, John G. Shedd Aquarium, 1200 South Lake Shore Drive, Chicago, IL 60605, USA. [6]Department of Marine Biology and Ecology, Rosenstiel School of Marine and Atmospheric Science, University of Miami, 4600 Rickenbacker Causeway, Miami, FL 33149, USA. [7]Hawaii Institute of Marine Biology, University of Hawaii, Kaneohe, HI 96744, USA.
*Corresponding author. Email: samuel.starko@gmail.com (S.S.); baum@uvic.ca (J.K. B.)

often show evidence of introgression, suggesting that they may have the potential to exchange adaptive genomic diversity (*27*, *38*). Although coral cryptic lineage complexes are common, the number of studies testing for differences in heat tolerance between cryptic lineages is limited (*39*, *40*). Moreover, heatwave studies of cryptic coral lineages tend to assess their bleaching tolerance [e.g., (*39*)], rather than their survival [but see (*23*)], despite the fact that these two processes can be decoupled (*41*). Consequently, climate change may already be threatening the persistence and coexistence of cryptic lineages, but the lack of genotype-specific time series data makes this problem challenging to detect. Quantifying differential mortality across cryptic coral genotypes, lineages, or species will therefore be essential to understanding and predicting the influence of future climate change on the diversity and adaptive potential of threatened coral reefs.

Although a handful of coral studies have tracked the stability of symbioses through marine heatwaves and shown that differential bleaching can strongly depend on algal symbionts (*11*, *39*, *41*), to our knowledge, only one has directly assessed the impacts of these events on the population genetics of coral taxa in natural systems (*23*). Moreover, despite growing awareness that cryptic coral lineages can harbor unique assemblages of symbionts, which could be the primary determinants of their climate change vulnerability (or resilience) [e.g., (*39*, *42*)], no study to date has simultaneously tested for shifts in both host population genetics and associated symbiont assemblages through an extreme heatwave event. Thus, while experimental work points to important functional differences between cryptic coral lineages (*40*, *43*, *44*), the extent to which heatwaves may be threatening particular cryptic lineages in nature remains unclear. Furthermore, given tight associations between some cryptic lineages and their symbiotic partners (*29*, *42*), it remains an open question how marine heatwaves alter symbiont specificity across co-occurring cryptic coral lineages, and if they potentially threaten rare or heat-sensitive lineages of either symbiotic partner (*11*, *45*).

Between 2014 and 2017, a series of heatwaves unfolded across much of the world's tropical reefs (*18*, *46*). This period, considered chronologically as the third global coral bleaching event on record, was unprecedented in terms of the severity, duration, and geographic spread (*46*). This event led to mass coral bleaching and mortality across many coral reefs in the Pacific and Indian Oceans, including extensive damage to the Great Barrier Reef (*18*, *41*, *47*, *48*). Species-level assessments of coral mortality have demonstrated that there were winners and losers in the face of this widespread bleaching, with survival varying substantially across coral taxa (*47*, *49*). However, it is not known whether differential survival during this global bleaching event affected the genetic composition of coral species or species complexes, nor how underlying local anthropogenic stressors—a feature of virtually all coral reefs—might modulate impacts on this critical facet of diversity.

Here, we directly assessed the extent to which marine heatwaves drive differential mortality across cryptic coral lineages and alter the specificity of host-symbiont pairings. We focused on one of the most widespread, ecologically important, and well-studied coral genera, *Porites,* and tracked the fate and algal symbiont composition of individual *Porites* colonies (massive growth form; identified in the field as *Porites lobata*) in the central equatorial Pacific Ocean, through the third global coral bleaching event. Within this region, the coral atoll Kiritimati experienced some of the highest levels of

accumulated heat stress ever documented on a coral reef, rivaled only by nearby Jarvis Island during this same time period (*49*). This heatwave lasted 10 months (June 2015 to April 2016), imposing up to ~31.6 degree heating weeks (°C-weeks) on Kiritimati's coral reefs (*41*). Despite this, massive *Porites* had relatively high survivorship (~80% at some sites), with highly variable bleaching severity and survival among colonies and sites (*49*). We leveraged this extreme climatic event as a natural experiment to directly test whether coral bleaching susceptibility or survivorship could be predicted by the genetic identity or lineage of the affected colonies and/or their associated algal symbionts. To accomplish this, we analyzed genetic data on colonies at two levels: tracking individual colonies (*n* = 79) from before to after the heatwave to directly compare survival, and analyzing a broader population-level sampling of massive *Porites* colonies before, during, and after the heatwave (*n* = 315 colonies total). Recent molecular studies have determined that the genus *Porites* comprises at least eight clades, some characterized by complex genetic structure (*28*, *50*), possibly reflecting cryptic or pseudo-cryptic lineages within each clade. Our study focused on one of these clades [clade V from (*50*); also known as the *P. lobata*/*lutea* clade] facilitating a deeper look into the functional differences between finer-scale cryptic lineages than has previously been achieved in this group. Our objectives were to examine (i) if cryptic coral lineages were present across Kiritimati, (ii) if survivorship of coral colonies varied across cryptic lineages or by their underlying exposure to chronic local human disturbance, (iii) if cryptic coral lineages were associated with specific symbionts and if there is evidence of host-symbiont coevolution (i.e., cophylogeny), and (iv) whether the specificity of these symbiotic partnerships was affected by mass bleaching and mortality during the heatwave.

RESULTS AND DISCUSSION
Sympatric cryptic lineages of *Porites*
We identified three genetic lineages of massive *Porites* (hereafter referred to as PKir-1, PKir-2, and PKir-3) that were found sympatrically across the reefs of Kiritimati before the 2015–2016 El Niño–driven heatwave (Fig. 1). Ordination [based on >12,000 single-nucleotide polymorphisms (SNPs) from 2b-RAD] revealed three distinct genomic clusters with no intermediate genotypes, which was further supported by ADMIXTURE analyses showing the lowest cross-validation (CV) error for $k = 3$, where every sample was assigned to a lineage with >85% probability (Fig. 1, A and B). Global F_{ST} values between lineages were also high, suggesting relatively high levels of differentiation across cryptic lineages (table S1). PKir-1 and PKir-2 (global $F_{ST} = 0.263$) were found to be more genetically similar to each other than either was to PKir-3 (global $F_{ST} = 0.361$ and 0.326, respectively; fig. S1). However, evidence for historical gene flow was detected between all lineages (fig. S2), suggesting that, although these lineages appear reproductively isolated in the present day, they have likely experienced introgression in the past.

Demographic analyses using Moments (*51*) based on allele frequency spectra (AFS) infer some limited gene flow between the three lineages with asymmetrical introgression across lineages and regions of the genome. The best-fit model supported the hypothesis of heterogeneous gene flow across the genome, with a small proportion of the genome experiencing particularly high gene flow (fig. S2). Moreover, we inferred higher gene flow from PKir-3 to PKir-
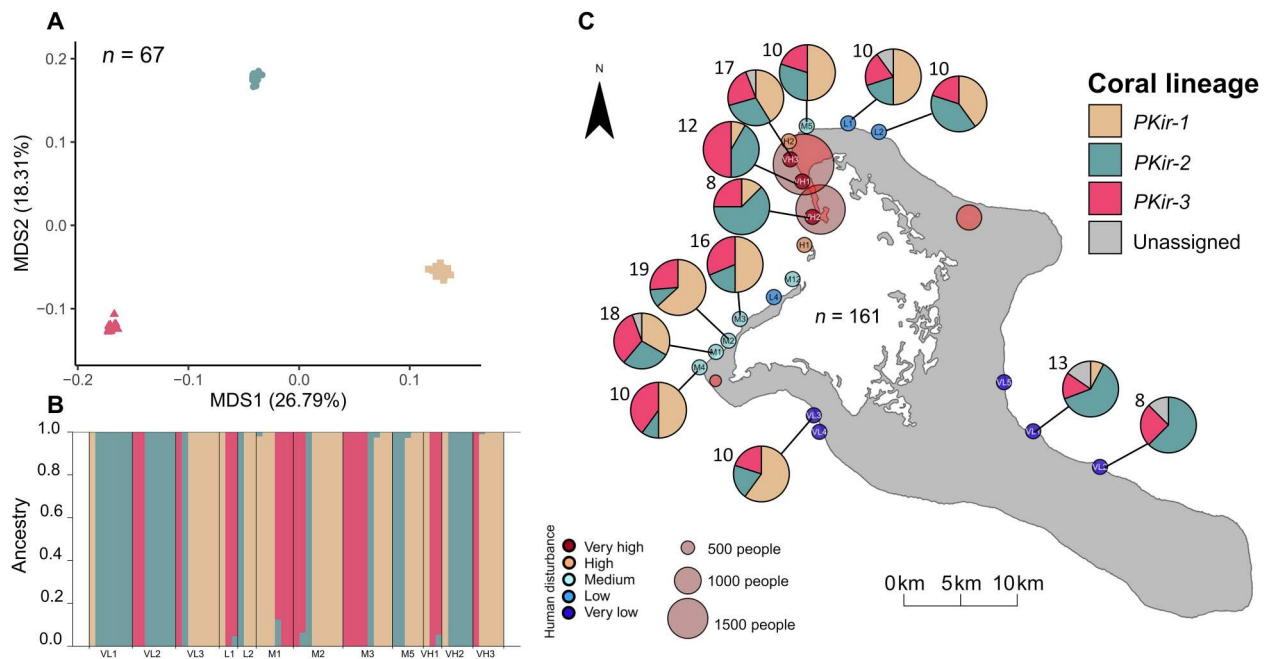
Fig. 1. Cryptic lineages of massive *Porites* across forereef sites on Kiritimati. (**A**) Principal coordinate analysis (PCoA) of 2b-RAD data (using 1-Pearson correlation matrices through ANGSD) showing three population clusters. (**B**) Results of ADMIXTURE analysis showing the assignment of colonies to one of three lineages, arranged by collection site. (**C**) Map with pie charts showing the relative abundance of each lineage at each site before the heatwave. Numbers indicate the number of colonies sampled and sequenced with either 2b-RAD or *ITS2* metabarcoding. Circles labelled with site names represent sites colored by level of human disturbance. Semi-transparent red circles indicate the location of villages, scaled by human population size.

1 and PKir-2 compared to the reverse direction (fig. S2). Analysis of one-dimensional AFS with StairwayPlot (*52*) revealed that effective population sizes (N_e) were similar across all three lineages, and all showed contractions in recent millennia (fig. S3).

Leveraging host sequences in the *ITS2* metabarcoding dataset, we were able to expand lineage assignment beyond the $n = 67$ colonies that were sequenced with 2b-RAD to $n = 300$ colonies, including all $n = 161$ colonies that were sampled before the heatwave (table S2). As expected, all *Porites* ITS2 sequences belonged to the same previously described *Porites* clade, clade V—the *P. lobata/lutea* clade (*50*) (fig. S4). However, examining colonies that were sequenced using both *ITS2* and 2b-RAD ($n = 67$), we found that host *ITS2* sequences were consistently dissimilar across the cryptic *Porites* lineages such that particular *ITS2* barcode sequences could be used to assign host lineages to those colonies not sequenced with 2b-RAD (see Materials and Methods). Using all samples collected before the heatwave for which lineage assignment was possible ($n = 157$ of 161), we found that, although the relative abundance of each *Porites* lineage varied across the atoll before the heatwave (Fig. 1C) (Fisher's exact test: $P < 0.001$), with significant differences between the southeast side of the atoll and other regions (fig. S5), lineage distribution was not driven by local human disturbance (multinomial regression: $\chi^2 = 1.5373$, $P = 0.4636$). We note that 1 colony out of the 79 with known survivorship (see below) could not be assigned to a lineage due to ambiguous *ITS2* sequences, indicating that it was from either PKir-1 or PKir-2.

Survivorship, cryptic host lineage, and human disturbance

Tracking individual colonies through nine time points that span the 2015–2016 heatwave, we found strong evidence of differential survival among lineages—an effect that was more pronounced at minimally disturbed sites (Fig. 2). Mortality of tagged colonies began during the heatwave (first observed in March 2016) and continued for at least a year following the heatwave, as colonies that had mostly died during the event finally experienced complete mortality in the months following the heatwave. We measured mortality (up to and including 2017) in two ways. First, we quantified colony mortality as a binary variable (died or survived, regardless of how much colony tissue remained) to determine whether colonies were eliminated from the population or remained to potentially grow and reproduce. Second, we examined variation in tissue loss across colonies, comparing the percentage of each colony that died from the heatwave (see Materials and Methods). We found that for both metrics, mortality varied significantly among lineages and levels of anthropogenic disturbance. Total mortality was greatest for PKir-3 (17 of 20; 85%) compared to the other two lineages (PKir-1: 16 of 30, 53%; PKir-2: 11 of 28, 39%) (Table 1; binomial regression—lineage: $\chi^2 = 12.2437$, $P = 0.0022$) and varied significantly with human disturbance (binomial regression—disturbance: $\chi^2 = 16.1409$, $P < 0.001$). This effect was driven by PKir-1 and PKir-2; while mortality was high across all values of human disturbance for PKir-3, total mortality sharply increased from 17 to 33% at minimally disturbed sites to 88 to 100% in PKir-1 and PKir-2 at sites exposed to very high human disturbance. Assessing tissue loss, we found that cryptic lineage and human disturbance were also significant predictors of this metric (quasibinomial logistic regression—lineage: $\chi^2 = 12.7531$, $P = 0.0017$, Disturbance: $\chi^2 = 8.7798$, $P = 0.0030$; Fig. 2B). For both metrics of survival, there were no significant interactions between lineage and human disturbance (binomial regression—lineage*Disturbance: $\chi^2 = 1.8726$, $P = 0.3921$;
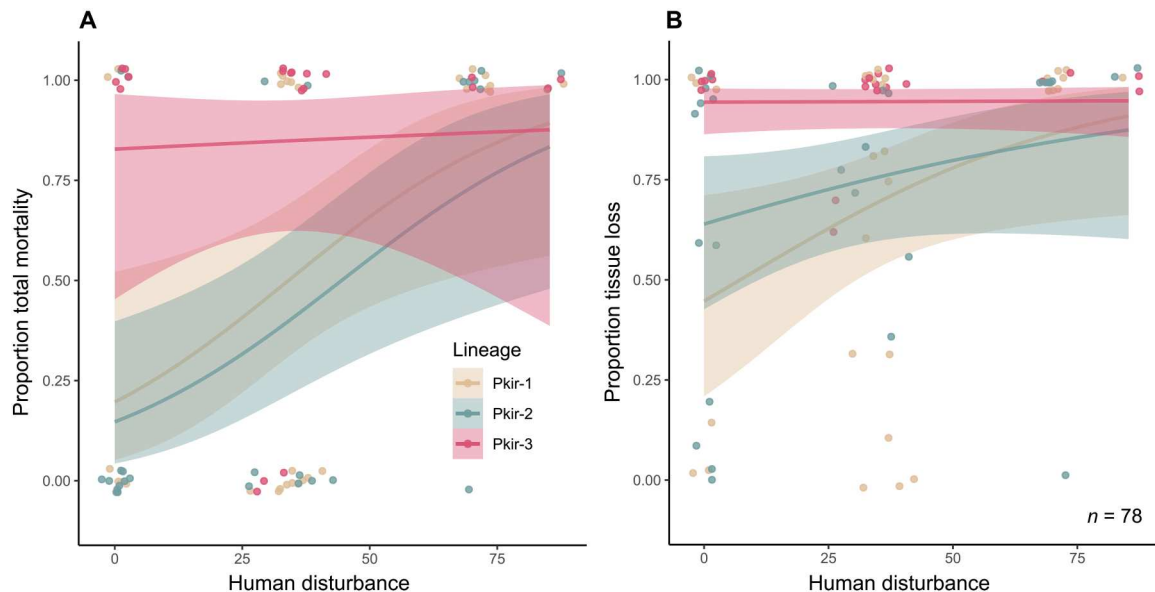
Fig. 2. Survivorship by coral cryptic lineage and chronic human disturbance. The probability that coral colonies experienced complete mortality between 2015 and 2017 (**A**) and the average percentage of partial mortality (i.e., tissue loss) that each colony experienced (**B**) both in relation to human disturbance and *Porites* lineage are shown. In (A), each point represents a colony that either survived (0) or died (1). The proportion of colonies that died at each value is estimated by the logistic regression line (shown with 95% confidence intervals). In (B), proportion mortality indicates the area of tissue loss experienced by each colony from 2015 to 2017, while each line shows the model fit with human disturbance for each lineage. Note that human disturbance is a relative metric based on fishing pressure and distance to Kiritimati's villages [see (*87*)]. Note that data points are jittered for visualization.

quasibinomial regression—lineage*Disturbance: $\chi^2 = 0.8086$, $P = 0.6674$), likely due to uncertainty in the effect of human disturbance on PKir-3.

We also found a significant effect of cryptic lineage identity on bleaching score using two different methods of categorizing bleaching (see Materials and Methods for description) such that PKir-3 tended to have the highest level of bleaching at both time points during the heatwave (2015—method 1: deviance = 7.8441, $P = 0.0198$; 2015—method 2: deviance = 11.303, $P = 0.0035$; 2016—method 1: deviance = 11.409, $P = 0.0033$; 2016—method 2: deviance = 13.155, $P = 0.0014$; fig. S6). There was no significant effect of colony size (area; cm^2) on survival through the heatwave, and lineages themselves did not differ in the size of colonies tracked through the heatwave (fig. S7). However, there was a trend toward a possible interaction between lineage and size [quasibinomial generalized linear model (GLM)—size*lineage: $\chi^2 = 5.8273$, $P = 0.0543$]. This was driven by increased survival (but not decreased tissue loss) in

larger colonies of PKir-1 and PKir-2, while PKir-3 had similarly high mortality across all colony sizes (fig. S7).

To explore the hypothesis that genomic differences may explain differences in heat tolerance, we tested for local genomic differentiation across the three *Porites* lineages and identified genes near outlier loci. While we found numerous genes near outlier loci when comparing lineage pairs (PKir-1 versus PKir-2: $n = 47$; PKir-1 versus PKir-3: $n = 63$; PKir-2 versus PKir-3: $n = 42$; file S1), the only gene near an outlier locus when comparing both PKir-1 and PKir-2 to PKir-3 matched the ETS-related transcription factor *Elf-2* (~57% similarity) with possible links to coral immunity (*53*), suggesting that genome-level functional differences may exist between cryptic *Porites* lineages.

Disruption of lineage-specific symbioses
We found strong associations between coral lineage and symbiont assemblage composition before the marine heatwave. Across all colonies sampled before the heatwave (i.e., population-level sampling),

Table 1. Survival and relative abundance of cryptic coral lineages before and after the 2015–2016 marine heatwave. Numbers indicate the number (and percentage) of colonies in each category.

| Lineage | Tagged colonies | | Population-level sampling | | |
	Survived	Died	Relative abundance before	Relative abundance after	Change in relative abundance
PKir-1	14 (47%)	16 (53%)	61/161 (38%)	84/173 (49%)	+29%
PKir-2	17 (61%)	11 (39%)	50/161 (31%)	64/173 (37%)	+19%
PKir-3	3 (15%)	17 (85%)	44/161 (27%)	16/173 (9%)	−77%
Unassigned	1	0	6/161 (4%)	9/173 (5%)	

there was a strong relationship between coral lineage and recovered C15-type *Cladocopium* sequence variants—i.e., variants of the *Cladocopium* C15 lineage [permutational multivariate analysis of variance (PERMANOVA): $F = 175.41$, $R^2 = 0.73$, $P < 0.001$]. Specifically, *Cladocopium* sequences formed two distinct clusters (Fig. 3, A and C), with variants in one cluster associating almost exclusively with PKir-3 colonies (all but one case, ~2.5%, although two PKir-3 colonies, 5%, also had symbiont sequences from the other cluster). This pattern was consistent across both maximum entropy decomposition (MED; Fig. 3A) and amplicon sequence variant (ASV; Fig. 3C) methods (see Materials and Methods), highlighting the robustness of these patterns to multiple analytical approaches. According to *ITS2* profile data output from SymPortal (*54*), which attempts to characterize putative Symbiodiniaceae taxa (by accounting for the multicopy nature of the *ITS2* locus), most of the coral samples taken at any time point (554 of 674 samples; 82%) were each characterized by a single C15-type *Cladocopium* profile (i.e., a profile from the C15 lineage), although profile identity was variable across colonies. Most of the remaining colonies (82 of 674 samples; ~12%) had mixed assemblages that included one C15-type profile and one or two additional profiles from other Symbiodiniaceae lineages (e.g., *Cladocopium* C116, C1, C3, *Durusdinium* D1, D4). A single sample had four associated profiles (including one C15-type). In total, we identified 47 C15-type profiles (110 profiles from all Symbiodiniaceae lineages) across all

colonies successfully sequenced. According to SymPortal, no corals were associated with more than one C15-type profile at a given time point and only ~3% (19 of 674) of samples lacked a C15-type profile altogether (mostly bleached colonies from March 2016; see below). Unlike PKir-1 and PKir-2, which initially associated with 9 and 13 profiles, respectively, PKir-3 had highly specific symbiotic associations before the heatwave, with 95% of colonies (38 of 40) associated with one of just three C15-type symbiont profiles that were absent or rare in other lineages (PKir-1: 0%, PKir-2: 3%). Moreover, all three of these *ITS2* profiles had the same dominant sequence [as identified using MED methods; referred to by SymPortal as "defining intragenomic variants (DIVs)"], suggesting that they reflect closely related symbiont populations. Specifically, PKir-3 tended to be associated with profiles that are dominated by the "C15cu" DIV, while the other two lineages tended to be associated with the "C15" DIV.

Leveraging the colonies that were sequenced using both 2b-RAD (host genomics) and *ITS2* metabarcoding (symbiont characterization), we tested for evidence of cophylogeny between symbiont and host lineages. There was a significant phylogenetic signal on the abundance of several *Cladocopium* DIV sequences (Moran's *I*: 22 of 31, 71%; Blomberg's *K*: 10 of 31, 32%; table S3) and *ITS2* profiles (Moran's *I*: 3 of 3, 100%; Blomberg's *K*: 1 of 3, 33% out of three profiles found in >10% of these samples; table S4), highlighting the specificity of symbiont sequences to particular host lineages. We
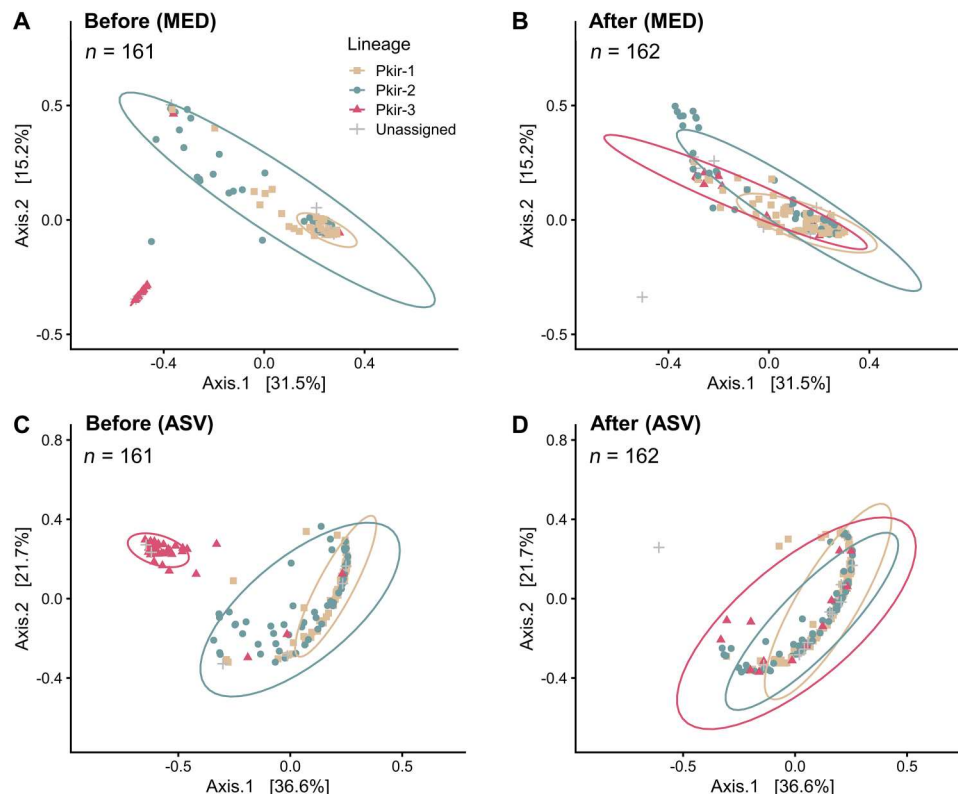

Fig. 3. Impact of the marine heatwave on lineage-specific symbioses. The results of PCoA based on unifrac dissimilarity of *Cladocopium* C15 maximum entropy decomposition (MED) sequences for all colonies sampled (**A**) before and (**B**) after the heatwave are shown. PCoAs based on Bray-Curtis dissimilarity of amplicon sequence variants (ASVs) from *Cladocopium* for each colony sampled (**C**) before and (**D**) after the heatwave are also shown. Ellipses at the 95% level are shown for each assigned coral lineage. Only samples with >500 sequence reads were included. Note that the ellipse for PKir-3 in (A) largely overlaps the points and is therefore challenging to visualize.

also performed procrustes analysis of cophylogeny (PACo) on data from these same colonies to test for cophylogeny between *Porites* and C15-type *ITS2* profiles. Given the multicopy nature of the *ITS2* locus, we used unifrac dissimilarities as a proxy for phylogenetic distance to produce a tree of C15-type profiles. Using a goodness-of-fit test, we found strong support for cophylogeny between massive *Porites* and their C15-type symbionts ($m^2_{XY} = 2.106617$, $P < 0.001$, $n = 10,000$; fig. S8). Together, these analyses support the hypothesis that cryptic lineages had coevolved, to some extent, with their symbiotic partners before the heatwave.

These tight relationships between *Porites* lineages and their *Cladocopium* symbionts were disrupted during the heatwave. Population-level sampling of colonies from after the heatwave indicated that the potentially coevolutionary associations between symbiont and host lineages were absent after the heatwave, with both MED and ASV sequences from all lineages forming a single cluster (Fig. 3, B and D). Following the heatwave, only one colony (whose lineage was unknown due to a lack of host sequence reads) was found to still have sequence variants common in PKir-3 before the heatwave. These patterns were also captured by analysis of *ITS2* profiles (figs. S9 to S13), where *C15cu ITS2* profiles (which were tightly associated with PKir-3 before the heatwave) were completely absent from PKir-3 colonies sampled after the heatwave ($n = 12$; Fig. 4). Symbiont assemblages across PKir-2 colonies also became more homogeneous, in general, with decreases in the relative abundance of colonies associated with profiles dominated by "*C15m*" and "*C15/C15cs*" DIVs in favor of colonies associated with profiles dominated by the *C15* DIV (Fig. 5 and figs. S9 to S13). This pattern is similar to a recent study on *Acropora* spp. showing losses in host-associated Symbiodiniaceae diversity at the reef scale during the same global bleaching event (*55*).

Approximately half of the colonies that were tracked for two or more time points (~51%; 80 of 158) had the same C15-type profile in every case; the remaining colonies hosted variable symbiont profiles over time (see Fig. 5 and fig. S9). Most notably, a few colonies sampled both before and after the heatwave appeared to recover from bleaching (observed in November 2016 or later) with a different C15-type profile. For example, one of the three surviving colonies of PKir-3 was associated with a *C15cu* profile (i.e., dominated by the *C15cu* sequence variant) before the heatwave but was later associated with a C15 profile (dominated by the C15 sequence variant) after the heatwave; the other two PKir-3 colonies that survived were not successfully sequenced with *ITS2*. Similarly, three PKir-2 colonies were associated with *C15m* profiles before bleaching (which were previously only found in that *Porites* lineage, PKir-2) and recovered from bleaching with C15 profiles. Notably, the *C15m* profiles were not found to dominate any colonies after the heatwave, despite their prevalence in PKir-2 before the heatwave. In all four colonies in which there were notable changes in C15-type profile identity, the initial symbiont profiles were completely absent in the colonies following their symbiotic shift. Moreover, all four colonies experienced turnover in the composition of DIVs, with some of the most common DIVs before the heatwave found to be absent following (fig. S14). Thus, shifts between *ITS2* profiles with different dominant DIVs (C15-type) appeared consistent with symbiont switching [i.e., symbiotic replacement by environmentally acquired symbionts (*31, 56, 57*)]. However, given that symbiont populations can be present in coral tissues at levels undetectable by metabarcoding methods (*58*) or may be present in different parts of the colony than were sampled (*59*), we cannot definitely differentiate between symbiont switching and shuffling [i.e., changes in relative abundance of two co-occurring symbionts (*56*)]. Some additional colonies (62 of 158) also appeared to shift between similar profiles (often sharing their most common DIVs but having additional minor sequence variants; e.g., *C15-C15ct-C15ch-C15cp-C15hj* versus *C15-C15ct-C15ch-C15cp-C15cq*). The overall similarity of these latter profiles (fig. S15) suggests that they may represent closely related members of the same symbiont population that may have even been assigned as different profiles due to sequencing artifacts (e.g., missing a rare sequence variant) rather than true biological differences. Alternatively, they may represent multiple co-occurring C15-type symbionts where the most common population is shared across time points. Because of this uncertainty in interpreting differences between similar symbiont
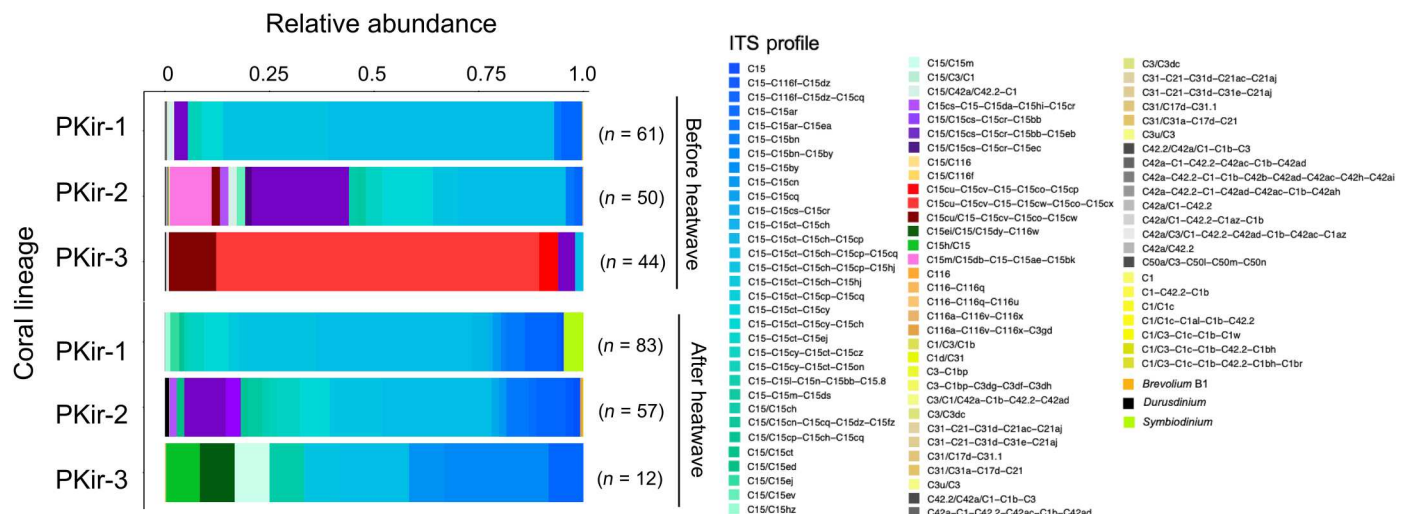
Fig. 4. The relative abundances of *ITS2* profiles across all colonies of each lineage before and after the heatwave. Sample sizes indicate the number of colonies. Only samples with >500 sequence reads were included.
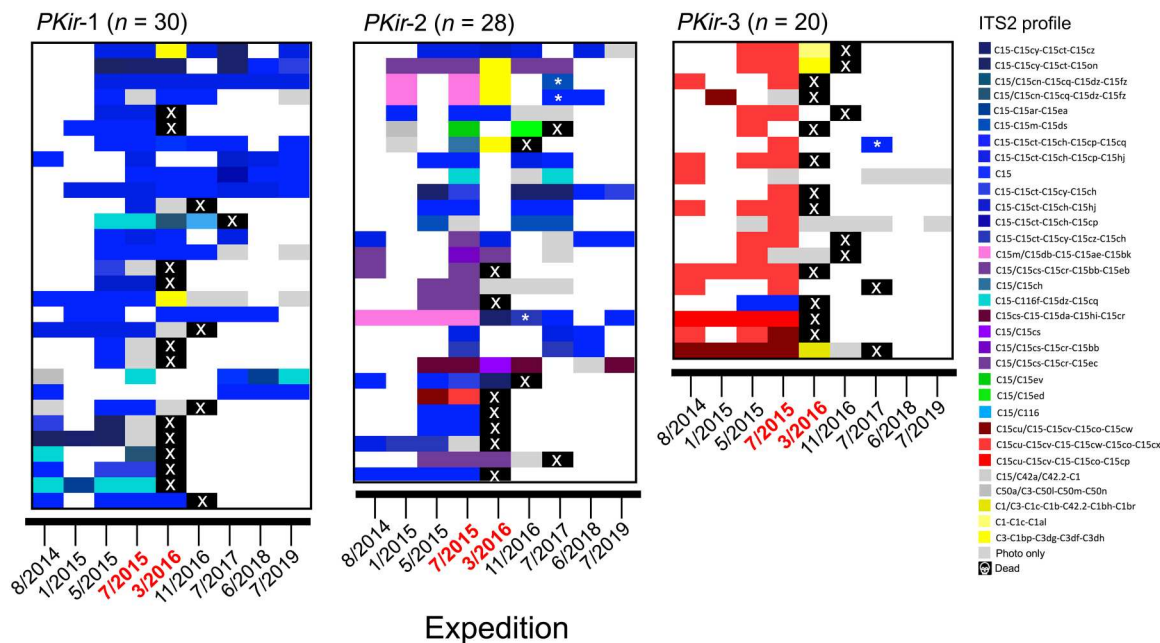
Fig. 5. Temporal stability of Symbiodiniaceae associated with tracked colonies of each cryptic *Porites* lineage. Each row represents an individual colony, with color at each time point indicating the most abundant symbiont profile. Colonies within each lineage are arranged in order of human disturbance (lowest on top, highest on bottom). Note that colonies that survived to 2017 were considered alive for survivorship analyses. Colonies that were considered to have switched between C15-type profiles (i.e., between *ITS2* profiles with different dominant DIVs; *n* = 4) are indicated with an asterisk. Expeditions during the heatwave are shown in red text.

ITS2 profiles, we only consider symbiont shifts between C15-type profiles when they differ in their most common DIV.

Late in the heatwave, several of the bleached colonies of all lineages were associated with *Cladocopium* C1- and C3-type *ITS2* profiles that were only ever present during that time point (March/April 2016; ~10 months into the heat stress; Fig. 5). In all cases, these colonies were severely bleached when sampled and all three surviving colonies that were sampled at later dates had recovered with symbionts characterized by C15-type sequence variants (see Fig. 5). Thus, due to the temporary nature of these three C1 and C3 profiles (1 —*C1/C3-C1c-C1b-C42.2-C1bh-C1br*; 2—*C1-C1c-C1al*; 3—*C3-C1bp-C3dg-C3-df-C3-dh*) on Kiritimati, we interpret these associations as transient Symbiodiniaceae infections, although we note that C1 and C3 symbionts have been found to stably associate with *Porites* spp. in other parts of the world [e.g., (*60*)]. So, while it remains unclear whether these C1- and C3-profile symbionts offered any benefit to bleached hosts, it is possible that they helped colonies maintain some basic nutritional requirements during the period between initial bleaching and subsequent recovery of C15-type symbionts. A similar pattern was observed during bleaching of *Pocillopora* spp. in the eastern Pacific, where bleached colonies were temporarily colonized by a presumed opportunistic *Breviolum* population (*11*). The functional and ecological importance of these short-lived symbioses remains unclear but offers an interesting avenue for future research. In our study, other symbiont types (e.g., C116 or *Durusdinium*) were generally rare and found inconsistently across samples, suggesting that these symbionts represent minor or opportunistic constituents of the *Porites* holobiont; they were not further examined here. However, we note that these rare profiles, although appearing only transient in massive *Porites*

on Kiritimati reefs, may still be of functional importance to the *Porites* holobiont.

Early studies assumed that massive *Porites* only acquired their symbionts vertically and therefore showed fixed symbiont dominance and high specificity (*61*). However, multiple studies have now shown that a single massive *Porites* colony can harbor mixed *Cladocopium* and *Durusdinium* communities (*62*, *63*) as well as different profiles from the C15 lineage (*59*). Thus, although vertical transmission occurs in *Porites* (and may be the dominant mode of transmission), these corals likely also have the ability to acquire new Symbiodiniaceae via horizontal transmission and/or "shuffle" dominant symbionts (*64*, *65*). Our data suggest that *Porites* can potentially associate with symbionts that have different *ITS2* profiles following extreme bleaching and can temporarily associate with C1- and C3-type symbionts. The ability to switch or shuffle symbionts is presumably adaptive by allowing corals to avoid evolutionary "dead-ends," whereby a vertically transmitted symbiont is fixed across the host population, but may be maladaptive under future warming (*31*, *57*). Laboratory experiments on *Montipora*, which also transmits its symbionts vertically, have shown that changes in symbiont assemblages acquired in one generation can be transferred to the next (*66*), providing an avenue for intergenerational plasticity in coral holobiont function (*67*). This suggests that the loss of variation in symbiont identity across colonies may persist for generations.

High degrees of vertical transmission and heritability in symbiont genotypes can lead to strong patterns of phylosymbiosis and/or cophylogeny (*68–70*), where closely related corals share similar algal symbiont communities, a pattern clearly reflected across host lineages in our dataset (fig. S16 and tables S3 and S4). Differences in symbiotic assemblages between cryptic lineages have

now been documented across multiple coral genera (*29*, *39*, *42*). Under strong selection from the heatwave, however, this pattern of co-occurrence between coral host lineage and algal symbiont sequence variants was disrupted in our study. The erosion of phylosymbiosis across coral lineages is likely driven largely by changing symbiont associations that occurred during recovery from bleaching. Among the tracked colonies, four (three from PKir-2 and one from PKir-3) that bleached and recovered post-heatwave did so with symbionts characterized by profiles that had different dominant DIVs than those they hosted before bleaching (all C15-type; Fig. 5). However, given that profiles dominated by the *C15* DIV were associated with ~5% of PKir-3 colonies before the heatwave (based on population-level sampling), differential mortality across colonies that had differing profiles initially (i.e., before the heatwave) may have also played a role in driving observed shifts in the population-level symbiont assemblages of each lineage. Consequently, although symbiont acquisition appears the most parsimonious explanation, the specific mechanism accounting for these symbiont changes cannot be unambiguously identified.

Although we lack the statistical power to definitively tease apart the role of symbiont from that of host lineage (due to high overlap among tracked colonies), the breakdown of host-symbiont associations and the observed switching between symbionts in 4 of 79 tracked colonies (5%) are most parsimoniously explained by fine-scale functional differences between some C15-type symbionts. In particular, we hypothesize that corals associated with symbiont profiles dominated by the *C15cu* DIV (and possibly the *C15m* DIV) are less thermally tolerant than those dominated by *C15* profiles. This hypothesis is further supported by the fact that all sampled colonies with less than 50% bleaching late in the heatwave (i.e., March/April 2016) were associated with *C15* profiles. This included the only two colonies assigned to PKir-3 that were not severely bleached when sampled during population-level sampling on that time point (fig. S6) and that were associated with *C15* symbionts despite the lineage being more typically associated with *C15cu* profiles. All colonies known to be associated with *C15cu* profiles before the heatwave bleached and experienced severe partial, or complete, mortality. Although functional differences between Symbiodiniaceae genera are well documented [i.e., *Cladocopium* versus *Durusdinium* (*41*, *57*, *64*, *71*)], it has remained unclear until recently whether more closely related symbionts (e.g., different C15-type variants) can confer functional variation on their hosts that is meaningful in the face of heat stress. However, recent work showed that *Porites cylindrica* and *Porites rus*—two clearly defined (i.e., both morphologically and genetically) species—differ in thermal tolerance and also associate with different C15-type symbionts (*72*). Moreover, variants of C3 in the Persian Gulf have rapidly evolved increased thermal tolerance relative to close relatives from nearby areas (*73*). Our study offers evidence in support of the hypothesis that some closely related algal symbionts can vary meaningfully in function (or confer differences in function on their hosts) by demonstrating how intense warming can result in the near-complete loss of a previously prominent symbiont type while increasing the relative abundance of its close relatives. Whether *C15cu* profiles are more thermally sensitive could be confirmed by using laboratory experiments or by continuing to track colonies of PKir-3 through the next major heatwave event, to test whether these colonies, having lost their association with *C15cu*, are now equally tolerant of heat stress as PKir-1 and PKir-2. In this way, remaining colonies

of PKir-3 may now be better suited to future heatwave events (*57*). However, if this is the case, then the beneficial response was confined to a minority of the PKir-3 population, with a mortality rate exceeding 80% and reductions in the overall relative abundance of that lineage (fig. S17).

Implications for cryptic complexes facing extreme events

Cryptic lineages are rapidly being uncovered across a broad range of taxa [e.g., (*36*, *74*)], but their functional importance remains unclear. Theory would predict functional differences between cryptic lineages if they have diverged as a result of ecological speciation (*75–77*), but close relatives tend to be ecologically similar when comparing to a broader pool of taxa (*78*). Thus, it remains unclear whether climate change has the potential to differentially affect cryptic lineages in nature, threatening their persistence in the face of environmental change. Here, we demonstrated that cryptic lineages can be disproportionately affected (and some threatened) by marine heatwaves. This finding has important implications for our understanding of how climate change is affecting the diversity of marine species and populations. Moreover, the decoupling of cryptic lineages from their distinct symbiont assemblages demonstrates that highly specific species interactions may also be threatened in the face of climate change.

Our inferred results would have differed substantially had we not characterized cryptic lineages in our study. While we would have still captured the major change in symbiont compositions that occurred during the heatwave, we would have missed the fact that the heatwave threatened a critical facet of diversity by disproportionately affecting one of the three cryptic lineages. While it is unclear whether *Porites* lineages represent early or incipient species or just highly differentiated populations, high (~80%) mortality across PKir-3 has the potential to threaten the long-term persistence of this lineage on Kiritimati. Given the widespread nature of cryptic diversity in corals and other habitat-forming species, we suggest that assessing the differential susceptibility of cryptic species or lineages to extreme events should be a major goal in the field of coral ecology and conservation. For example, differential success of distinct *Pocillopora* lineages that vary in their ability to associate with heat-tolerant symbionts (*Durusdinium glynni*) has recently been implicated in the long-term persistence of coral reefs in the eastern tropical Pacific (*79*). Some of the paradigms that underlie our understanding of population and species-level ecology (e.g., variation in traits, performance, and survival) could be reconsidered in light of cryptic diversity (*74*).

We also found that human disturbance increased the susceptibility of tagged colonies to heatwave-driven mortality. While the interaction between human disturbance and coral lineage was not significant using either metric of mortality, it is noteworthy that mortality appeared equally high across all lineages on highly disturbed reefs, despite clear differences in mortality at lower disturbance sites (Fig. 2). Past work has found that human disturbance can have either negative (*41*, *49*) or positive effects (*80*, *81*) on coral thermotolerance or survivorship through heatwaves and this has been linked to disturbance-driven changes in the symbiont composition (*41*, *81*) or density (*80*). Here, we found negative impacts of human disturbance irrespective of symbiont community composition (figs. S10 to S12). Overall, our results suggest that, for *Porites*, human disturbance negatively affects survivorship through heatwaves, regardless of cryptic host lineage or symbiotic associations. Moreover,

given differences in survivorship between high and low disturbance sites for PKir-1 and PKir-2, our results demonstrate that the combined impacts of human disturbance and prolonged thermal stress may exceed the tolerance of even putatively stress-tolerant lineages. Thus, while the preservation or future-proofing of undisturbed reefs may benefit from the use of stress-tolerant genotypes or lineages [see, e.g., (67, 82)], these types of efforts may have less impact in highly disturbed areas.

Limitations of study

Although our research provides important insights into the impacts of heatwaves on cryptic diversity of reef-building corals and their symbiotic partners, its limitations may serve as interesting avenues for future research. In particular, it is challenging to directly tease apart the impacts of host genetics from those of symbiont identity in our system given that these nearly completely overlapped before the heatwave (see Figs. 3 to 5). While various patterns support the hypothesis that fine-scale differences between some C15-type symbiont populations explain some of the observed patterns in differential mortality and abundance, host genetics may also play a role. For example, we identified one gene that was an outlier between PKir-3 and both PKir-2 and PKir-1: ETS-related transcription factor *Elf-2*, which may have possible links to coral immunity (53). Thus, it is possible that genetic differences between these cryptic lineages influenced the probability of survival, for example, by increasing bleaching propensity or susceptibility to disease following bleaching. Further experimental work or colony tracking of massive *Porites* lineages is required to definitively tease apart the role of host versus symbiont genetics in bleaching susceptibility or survival. Given the widespread nature and ecological role of *Porites* spp. on coral reefs globally, this offers a potentially critical direction for future investigation.

Other limitations involve our ability to track all colonies and assign them to their respective cryptic lineages due to challenges (e.g., weather and safety) associated with tagging corals on remote reefs. Moreover, even when colonies were tracked, sequencing sometimes failed or samples were not taken because the surviving tissue area was deemed too small, leaving gaps in our knowledge of host lineage or symbiont identity. For example, two of the PKir-3 colonies that survived the heatwave could not be sequenced following the event. These colonies both bleached and experienced substantial partial mortality during the event; thus, it would be informative to know which symbionts they associated with after the event. Nonetheless, consistent patterns between tracked colonies and population-level sampling before and after the heatwave suggest that symbionts closely associated with PKir-3 before the heatwave were virtually absent afterward. Another limitation lies in our use of both 2b-RAD and coral *ITS2* sequences to assign colonies to their respective lineages. While this multi-method approach allowed us to substantially increase replication, there are associated limitations. First, a number of colonies could not be assigned to a coral lineage because they had *ITS2* barcode sequences that were ambiguous or did not match a reference sequence from the colonies also sequenced with 2b-RAD (n = 15 colonies; see Materials and Methods). It is likely that these latter colonies are members of the three lineages but have *ITS2* variants that were not represented in the colonies sequenced with 2b-RAD (n = 67) by chance. Second, there is a higher risk of false lineage assignment when using barcoding rather than genomic data to assign colonies

to cryptic lineages, although we note that barcoding sequences are commonly used to assign cryptic lineages or species [e.g., (36, 42)]. Introgression or incomplete lineage sorting, for example, could lead to a misleading pattern when looking at a single locus [e.g., (83, 84)]. Misassignment is probably more likely between PKir-1 and PKir-2 than between either one and PKir-3, based on the distribution of *ITS2* barcodes across colonies sequenced with both methods (figs. S18 and S19), and due to the close affiliation of PKir-1 and PKir-2 in the genomic data. Thus, our conclusions about PKir-3 relative to the other two lineages should be robust to errors introduced by misleading barcode sequences. Nonetheless, as a sensitivity test, we tested whether cryptic lineage predicted survivorship using only the subsample of colonies sampled with 2b-RAD and with known survival (n = 61) and found similar overall statistical results (fig. S20).

Finally, our study focused on only a single depth range; thus, the full distributions of these cryptic lineages remain to be characterized. Although all three *Porites* lineages were sympatric across Kiritimati, the extent to which they fully overlap across the seascape remains unclear. Past work on cryptic lineages has demonstrated that they often inhabit discrete microenvironments even if they do overlap over broader spatial scales [e.g., (30, 39)]. While depth was standardized across sites and tagged colonies (see Materials and Methods), it is possible that asymmetrical gene flow inferred across lineages could be the result of differences in habitat. For example, if PKir-3 is found across a larger range of habitats than the other two lineages, this could help to explain why gene flow was reduced into PKir-3. Given the functional differences in thermal tolerance through a major heat stress event, it is possible that these lineages generally occupy different depth ranges but co-occur in the moderate forereef environment where we sampled [as observed in *Pocillopora* spp. in Mo'orea (42)]. Understanding the distribution of cryptic coral lineages across different environments will be important for elucidating the processes driving and reinforcing differentiation across these lineages and for better predicting the outcomes of future bleaching events (27).

Summary

By coupling host genomic sequencing and Symbiodiniaceae metabarcoding with longitudinal coral colony tracking, we showed that differential mortality during a marine heatwave resulted in a substantial change in the relative abundances of cryptic lineages of massive *Porites*, with a relative decrease of ~80% in one lineage (PKir-3) across the atoll following the heatwave (Table 1). This provides direct evidence that heatwaves have the potential to threaten cryptic genetic diversity, even among one of the most common and stress-tolerant coral genera. These cryptic *Porites* lineages had specific symbiont associations that recombined during the heatwave, highlighting a likely mechanism behind differential survival of lineages. Moreover, mortality was strongly predicted by human disturbance but only in two of the three cryptic lineages, illustrating that anthropogenic drivers can mediate the strength of selection during extreme events. High mortality in PKir-3 decreased its overall population size, increasing the probability that this lineage may be extirpated in the future. Although changes in symbiont associations in this lineage may facilitate adaptive change (31) in the face of future heatwaves, with unknown functional trade-offs (57), the loss of this specific host-symbiont pairing demonstrates how heatwaves may be eroding specific biotic interactions in addition

to threatening diversity. Our study demonstrates that strong marine heatwaves may threaten biodiversity at finer scales than have generally been appreciated to date. Overall, these findings underscore the need to better understand cryptic diversity within our current taxonomic framework. They also illustrate how climate change may threaten the persistence of undiscovered diversity, causing Centinelan extinctions—losses of taxa that are never described by science and are therefore unrecorded (85). Moreover, this undescribed diversity may help explain enigmatic variation in coral bleaching and mortality, and improve future predictions of bleaching severity and impact.

MATERIALS AND METHODS
Study location and design
Kiritimati (Christmas Island), Republic of Kiribati, is located in the central equatorial Pacific Ocean (01°52′N 157°24′W), at the center of the Niño 3.4 region (a delineation used to quantify El Niño presence and strength). Kiritimati is the world's largest atoll by landmass (388 km^2; 150 km in perimeter), and all 18 surveyed reefs surrounding the atoll are sloping, fringing reefs with no back reef or substantial reef crest formations. Kiritimati has a strong spatial gradient of human disturbance, with most of the human population restricted to two villages on the northwest side of the atoll. Human uses, including wastewater runoff, subsistence fishing, and a large pier, are densely concentrated in this area, while other parts of the atoll experience substantially less human disturbance. The intensity of chronic local human disturbance at each site has previously been quantified, using two spatial data sources: (i) human population densities and (ii) fishing pressure (41, 49). First, as a proxy for immediate point-source inputs from villages into the marine environment such as pollution and sewage runoff, a geographic buffer (in ArcGIS) was generated to determine human population size within 2 km of each site. Nearly all people live in villages, and village location was mapped based on published field surveys. Population size for each village was extracted from the 2015 Population and Housing Census from the Kiribati National Statistics Office (86). Second, to account for the more diffuse effects of subsistence fishing on the reef ecosystem, a kernel density function with 10 steps was generated based on mapped fishing intensity from household interviews conducted by Watson et al. (87). Each metric was weighted equally, and from this, combined metric sites were grouped into five distinct disturbance categories, termed very low, low, medium, high, and very high. For all quantitative analyses, human disturbance was treated as a continuous variable by square root–transforming the combined metric to account for skew in the data [as in (41)].

Coral tagging and sampling
We tagged and sampled colonies of massive Porites along 60-m transects, laid along the 10-to-12-m isobath, at each of the 18 different fore reef sites around Kiritimati (Fig. 1C), on expeditions before (August 2014, January/February 2015, April/May 2015), during (July 2015, March/April 2016), and after (November 2016, July 2017, June 2018, July 2019) the 2015–2016 El Niño–driven heatwave. All colonies were identified in the field as P. lobata. Twelve of the sites were sampled both before and after the heatwave; one site was sampled before but could not be accessed after, and five of the sites were sampled only after the heatwave. In total, 315

massive Porites colonies were included in this study from at least one time point on the basis that symbiont and/or host lineage was obtained from sequence data (detailed below). An additional two colonies, sampled at a single time point, were excluded due to presumed contamination on the basis that they lacked sequence reads matching Porites spp. and had unusual symbiont assemblages, more typical of favidae or merulindae. At each visit, each coral colony was photographed and a tissue sample was taken, except in the few cases following the heatwave when the live tissue remaining on the colony was too small to sample.

Of the total set of colonies included in this study (n = 315), 161 colonies were initially tagged and sampled before the heatwave (n = 6 to 20 at 13 sites). However, not all sites could be visited during each expedition, and some site surveys were only partially completed during some expeditions due to unfavorable weather conditions or other logistical constraints. Among these 161 colonies, we were able to track the survivorship of 79 through the mortality event (3 to 10 per site) on the basis that tagged colonies could be relocated at various time points spanning the heatwave. All but one of the tracked colonies (n = 78) were assigned to a cryptic Porites lineage using either 2b-RAD sequencing or host ITS2 metabarcoding data (see below). Several additional colonies were sampled only during (n = 5), after (n = 103), or during and after (n = 46) the mortality event. Some colonies were sampled but sequences could not be obtained due to sample quality and/or failed benchwork.

Assessing bleaching and mortality of tagged colonies
We considered mortality in two ways. First, whether a colony experienced total mortality (i.e., no living tissue remaining) or not. This was meant to capture changes in relative abundance of individual colonies of each lineage and was a binary measure (0 = alive, 1 = dead). We also looked at the proportion of each colony that was lost through either partial or complete mortality—tissue loss (0 = no mortality, 1 = complete mortality). Mortality from bleaching began some time following the July 2015 expedition and continued until at least late 2016 but ceased following the July 2017 expedition (Fig. 4). Thus, we considered a colony to have died (i.e., total mortality) if its mortality was recorded between March 2016 and July 2017 expeditions, and we considered colonies to have survived if they were found alive in 2017 or later. None of the 79 colonies tracked through the heatwave died later than 2017, but some were not tracked beyond that time point. To assess tissue loss (i.e., proportional mortality), the surface area of each colony was approximated before the heatwave using photos and analysis with ImageJ (U.S. National Institutes of Health, Bethesda, MD, USA) and compared to similar surface area estimates following 2017 or later (using first available image). We also used the initial surface area estimates of these tracked colonies (n = 79) to assess differences in colony size between lineages (see below). All other colonies were not included in survivorship analyses but provide additional insight into the relative abundance of different coral lineages and symbiont sequence variants across the various expeditions. Because symbionts remained stable and no mortality had yet occurred at the early time point in the heatwave (July 2015), we considered all 2015 surveys to have occurred before the mortality event and thus included these samples as "before heatwave." Overall, sample sizes of each analysis vary depending on the number of colonies for which necessary information (e.g., host lineage, symbiont sequence variant, and survivorship) were available (tables S5 to S8).

Bleaching was assessed visually from photographs of each colony, using categorical scores based on the percentage of the colony that was visually bleached. Given challenges associated with classifying bleaching into discrete categories, we used two different schemes to ensure that results were robust to methodological choices. We used the categories of Baum *et al.* (*49*) and Claar *et al.* (*41*)—hereafter method 1—which includes three categories from healthy to severely (>80%) bleached: (i) no bleaching, (ii) small patches of bleaching <5 cm or paling to 50% of colony area, (iii) bleaching in patches >5 cm or more than 50% of colony pale, and (iv) severe or complete bleaching (>80%) or entire colony pale. We also used the categories of McClanahan (*88*)—hereafter method 2—which includes six categories from healthy to completely (100%) bleached: (i) no bleaching, (ii) paling or discoloration, (iii) 0 to 20% bleaching, (iv) 21 to 50% bleaching, (v) 51 to 80% bleaching, and (vi) 81 to 100% bleaching. Given that many colonies had already experienced partial bleaching-induced mortality by March 2016 (due to the extreme length of the heatwave), we assumed that partial mortality of bleached colonies was the result of bleaching and therefore grouped partial colony mortality and bleaching together for both bleaching metrics. For example, a colony with 50% mortality but only 10% bleaching of remaining tissue would be assigned a "3/4" and a "5/6" for the Baum *et al.* (*49*) and McClanahan *et al.* (*88*) methods, respectively.

DNA extraction
We performed DNA extractions using two methods. First, a guanidinium-based extraction protocol optimized for Symbiodiniaceae DNA (*56*, *89*) was used for all extractions sequenced for *ITS2* metabarcoding. Second, we used the DNeasy Blood and Tissue kit performed with modifications to optimize for coral genomic DNA extraction (*90*) for most samples sequenced using 2b-RAD since this protocol is known to yield high–molecular weight genomic DNA necessary for genomic-level sequencing. In a few cases (*n* = 4), there was not enough remaining tissue from a given sample to perform the DNeasy method. In these cases, the guanidinium extraction was used for both *ITS2* metabarcoding and 2b-RAD. Following the guanidinium protocol, the DNA pellet was washed with 70% ethanol three times rather than once and, if necessary, the final product was cleaned using Zymo Genomic DNA Clean and Concentrator-25 (catalog nos. D4064 and D4065) following the standard protocol (http://www.zymoresearch.com/downloads/dl/file/id/638/d4064i.pdf) to isolate clean, high–molecular weight DNA. This was especially necessary when sequencing guanidinium extracts with 2b-RAD.

High-throughput sequencing
We used amplicon sequencing to characterize the algal symbiont communities associated with each coral colony. We chose the *ITS2* amplicon for high-throughput sequencing because it is currently the standard region used for identification and quantification of Symbiodiniaceae taxa (*54*). Library preparation for Illumina MiSeq *ITS2* amplicon sequencing was performed following the Illumina 16S Metagenomic Sequencing Library Preparation (Illumina protocol, part # 15044223 Rev. B) with the following modifications: (i) *ITS2* primers (ITSD-forward: 5′-TCGTCGGCAGCGTCAGATGTGTATAAGAGACAGGTGAATTGCAGAACTCCGTG-3′ and *ITS2*-reverse: 5′-GTCTCGTGGGCTCGGAGATGTGTATAAGAGACAGCCTCCGCTTACTTAT

ATGCTT-3′) were used in place of the 16S primers. (ii) Polymerase chain reaction (PCR) 1 annealing temperature was 52°C, PCR 1 was performed in triplicate, and PCR product was pooled before bead clean. (iii) A 1:1.1 ratio of PCR product to SPRI beads was used for PCR 1 and PCR 2 cleanup. Samples were sequenced on the Illumina MiSeq platform at Hawai'i Institute of Marine Biology Genetics Core Facility or Shedd Aquarium's Molecular Ecology Laboratory, which yielded 2 × 300 base pair paired-end reads.

Extracts from *n* = 67 samples were prepared for 2b-RAD sequencing following the methods of Wang *et al.* (*91*). These samples were intended to cover a range of sites while focusing on the colonies for which survivorship was known. However, there was not enough tissue or DNA remaining to include all samples. Eight replicate samples were prepared to identify clones (none were found in this dataset). Samples were barcoded, multiplexed, and sequenced across two lanes of Illumina HiSeq 2500 at Tufts University Core Facility (TUCF). Raw reads were trimmed, deduplicated, and quality-filtered with FASTX TOOLKIT (http://hannonlab.cshl.edu/fastx_toolkit), and only reads with Phred scores >20 were maintained (-q 20 -p 100). Quality-filtered reads were first mapped to a concatenated genome of four Symbiodiniaceae genera *Symbiodinium*, *Breviolum*, *Cladocopium*, and *Durusdinium* (*92*–*94*) via bowtie2 (*95*). Any reads that mapped successfully with a minimum end-to-end alignment score of −22.2 were removed so that those left behind could be assumed to be absent of symbiont contamination. The remaining reads were then mapped to the *Porites lutea* genome (*96*). Genotyping and identification of SNPs was performed using ANGSD v0.921 (*97*). Standard filtering that was used across all analyses included loci present in at least 80% of individuals, minimum mapping quality score of 20, minimum quality score of 25 [unless no minimum allele frequency (MAF) filter was used, in which case quality scores of 25 and 30 were used], strand bias *P* value >0.05, heterozygosity bias >0.05, removing all triallelic sites, and removing reads having multiple best hits and lumped paralogs filter (see file S2 for proportion of missing data for each analysis). Raw sequence data are available on the National Center for Biotechnology Information (NCBI) Sequence Read Archive under PRJNA869749.

Analysis of algal symbiont communities
Symbiodiniaceae communities were inferred via *ITS2* sequence data using two analytical approaches: (i) ASV clustering and assignment in dada2 (*98*) and (ii) SymPortal, implemented through the online portal (*54*). To analyze ASVs, sequence files were run through the dada2 pipeline (*98*) in R using a reference database that included both Symbiodiniaceae and *Porites ITS2* sequences (taken from GenBank). ASVs assigned to *Cladocopium* were then stored in a phyloseq (*99*) object and used in subsequent analyses. ASVs assigned to *Porites* were also stored in a separate phyloseq object and used for downstream host lineage assignments.

In contrast with ASV methods, SymPortal first uses a MED approach to assign sequence variants (hereafter MED sequences) and then combines them into "*ITS2* profiles" that are intended to represent groups of sequences shared by the same organism (i.e., intragenomic sequence variants). From SymPortal results, analyses were conducted (and visualizations were produced) using both the *ITS2* profile matrix and the MED sequence variant matrix output directly from SymPortal. We note that MED sequences include not only DIVs, the sequences that make up the *ITS2* profiles, but also rarer

sequences that are not incorporated into *ITS2* profiles (*54*). Between-sample unifrac dissimilarity matrix was also output from SymPortal and used as part of the coevolutionary analysis (see below). To produce evolutionary trees for unifrac-based ordinations of the DIV matrix, sequences were aligned in Geneious (*100*) and an NJ tree was produced using a Tamura-Nei substitution model.

Lineage assignment

To detect population structure among corals from all sites, the program ADMIXTURE v. 1.3.0 (*101*) was used to find the optimal number of clusters (*K*) with the least CV error. SNPs were hard called using genotype likelihoods estimated by SAMtools with an SNP *P* value of <0.05 (12,755 loci). Principal coordinate analyses (PCoAs; using 1-Pearson correlation) were performed using a covariance matrix based on single-read resampling calculated in ANGSD, and admixture results were visualized using the *K* with the least CV error reported from ADMIXTURE and the most likely *K* based on principal components analysis (PCA). Samples were assigned to lineages based on the >0.85 assignment to a single lineage in ADMIXTURE and segregation along PC1 and PC2 axes in PCoA space. Example photographs of each lineage are provided in fig. S21.

Following lineage assignment using the 2b-RAD data, we used host contamination in the *ITS2* metabarcoding data (i.e., ASVs assigned to *Porites*) to further assign additional colonies to each lineage using a DNA barcoding approach. *Porites ITS2* sequences were consistently dissimilar across lineages (with one exception) when assessing samples assigned to lineage using 2b-RAD, indicating that defining sequence variants (i.e., barcodes) could be effectively used to assign colonies to lineage using *ITS2* data alone. ASVs matching *Porites* from the dada2 output (see above) were isolated, and the dominant ASV (for homozygous; at least 97% relative read abundance) or top two ASVs (for heterozygous; at least 40% relative abundance for second most abundant sequence) found in each coral were treated as DNA barcodes and used to assign lineages for samples not sequenced using 2b-RAD. For colonies that had ambiguous sequences (i.e., shared by PKir-1 and PKir-2) or sequences that did not match reference sequences obtained from the colonies also sequenced with 2b-RAD, lineage assignment was not possible (*n* = 15). We also compared *Porites ITS2* ASVs to reference sequences in GenBank and constructed neighbor-joining trees in Geneious Prime (*100*) to determine how the three lineages identified in this study compare to previously described *Porites* clades (*28*, *50*).

The set of *Porites ITS2* sequences found in each cryptic lineage was paraphyletic relative to the sequences of other lineages (figs. S4 and S6 and table S8), likely reflecting the recent reticulate divergence of these cryptic lineages and confirming that this clade consists of a cryptic complex rather than a single, highly plastic species [see discussion in (*28*)]. In total, 36 dominant *Porites ITS2* sequence variants were present across the 67 colonies sequenced with both metabarcoding and 2b-RAD. Of these, 28 sequences were also found across the other colonies in the dataset and were thus used as barcodes to assign lineages. One dominant sequence variant was found in both PKir-1 and PKir-2, making it uninformative for lineage assignment. However, this sequence variant was relatively rare across the dataset (*ASV9*: 23 of 315—7% of colonies). Several uncommon *ITS2* sequence variants (*n* = 7) were not found in any samples assigned using 2b-RAD, preventing lineage assignment of colonies that had them. In total, we were able to assign 95% (300 of 315) of colonies included in this study using either 2b-RAD or *ITS2* metabarcoding data. Of the 5% remaining colonies, ~1% (4 of 315) were unassigned due to unknown sequences (i.e., those not present in 2b-RAD samples), ~2% (7 of 315) were unassigned due to the dominance of the ambiguous sequence shared by two lineages (and are therefore from either PKir-1 or PKir-2), and ~1% (4 of 314) were unassigned due to a lack of sequence reads altogether. Unassigned colonies were excluded from analyses comparing cryptic lineages.

Testing hypotheses of host-symbiont coevolution

Leveraging colonies that had been sequenced with both 2b-RAD and *ITS2*, we tested for cophylogeny between *Porites* colonies and their *Cladocopium* symbionts using three different methods. For all three methods, we used outputs from SymPortal (MED sequences and *ITS2* profiles) to characterize symbiont assemblages. First, we tested for a phylogenetic signal on individual C15-type MED sequence variants by using a phylogenetic tree produced for these colonies and calculating Moran's *I* and Blomberg's *K* for each sequence separately. Second, we did the same tests but using *ITS2* profiles. For both of these analyses, we used Benjamini-Hochberg (BH) corrections for multiple comparisons and excluded variants that were present in <10% of samples (leaving 31 MED sequences and 3 *ITS2* profiles). Because only common sequences were included in the first analysis, all MED sequences analyzed in this regard were considered DIVs by SymPortal. Third, we used PACo implemented in the R package "paco" (*102*) to test for cophylogeny between the colony-level *Porites* phylogeny and a symbiont *ITS2* profile tree constructed using unifrac dissimilarity as a distance metric. In all analyses, we used a maximum likelihood phylogeny of *Porites* colonies, which was inferred in RAxML (*103*) using neutral loci (see below) and an SNP *P* value of 1×10^{-5} and a MAF filter of 0.05. A GTRGAMMA model and 100 rapid bootstraps were used along with the resulting concatenated sequence matrices.

Analyses of genetic divergence and demographics between lineages

BayeScan v. 2.1 (*104*) was used to identify a set of putatively neutral loci. The F_{ST} outlier method implemented in BayeScan identified outliers using 5000 iterations, 20 pilot runs with length 5000, and burn-in length of 50,000. We used the default prior odds of neutrality (*10*) and a *q*-value cutoff of 0.50 after false discovery rate (FDR) correction for removing all putatively nonneutral loci. To determine genetic differentiation between lineages, ANGSD was used to calculate the site allele frequency (SAF) for each lineage using no MAF filter (363,736 loci) and neutral loci only and then realSFS calculated the site frequency spectrum (SFS) for all possible pairwise comparisons. These SFSs were used as priors with the SAF to calculate global F_{ST}. Here, only weighted global F_{ST} values between lineages are reported. ANGSD was used to obtain 100 series of five block-bootstrapped SFS replicates, which were averaged to create 100 bootstrapped SFS for each lineage. SFS was polarized using the *P. lutea* genome as an ancestral reference. Multimodel inference in Moments was used to fit two-population models [https://github.com/z0on/AFS-analysis-with-moments (*105*)], and all unfolded models were run on 10 bootstrapped SFS and replicated six times. The best-fit model was then selected based on lowest AIC (Akaike information criterion) value. Parameters [i.e., migration, epoch times, and effective population sizes (*N*_e)] for the best-fit model

were obtained by running the best-fit model on 100 bootstrapped SFS and replicated six times. Additionally, we ran the unsupervised analysis StairwayPlot v2 (*106*) to one-dimensional SFS as a second effort to reconstruct effective population sizes. For all demographic analyses, we used a mutation rate of 1.38×10^{-9} [from the 0.138% per million years substitution rate in Prada *et al.* (*107*) calculated for the *Porites* genus] per base per year and generation time of 6 years. The generation time was calculated from the average reproductive colony size of *P. lutea* [8-cm diameter; (*108*)] and average growth rate of 1.3 + 0.3 cm/year for *P. lobata* (*109*). Note that adjusting the generation time should have no impact on the interpretation of the results beyond affecting age values. Relative population sizes and introgression estimates should be robust to changes in generation time. Nonetheless, we ran the StairwayPlot analyses using two other generation times to ensure that this was the case (18 and 35 years; see figs. S22 and S23). Small variation in historical N_e between runs with different generation times was due not to changing the generation time but rather to the variation in N_e estimation that occurs with random subsampling of the AFS. Regardless, trends in the last 500 ka (thousand years) were consistent across all three generation times.

Identifying genes under selection across lineages

Additional filtering of loci was conducted before outlier analyses, which included SNP *P* value 1×10^{-5} (SNPs were hard called for this analysis) and MAF < 0.05 (4956 loci). Our data were subset to include only two pairs of lineages for each comparison. The aim of this approach was to isolate outlier loci between the PKir-3 and versus both PKir-1 and PKir-2 to look for candidate genes that might explain the differential mortality outcomes. First, PCAdapt v. 4.3.3 (*110*) was used to determine the optimal *K* for all pairwise comparisons using a score plot displaying population structure. A *K* of 2 was selected for all pairwise comparisons between all lineage pairs, and *P* values were extracted from PC1, which separated each lineage pair. We performed an FDR correction on these *P* values to create converted *q* values, which were transformed using a BH correction to account for the multiple comparisons between lineages. A *q* value of 0.05 was used as a cutoff for determining outlier loci, and annotated genes [using the annotation file from (*111*)] 1 kb upstream or downstream of this outlier locus were reported.

Statistical analyses

For all statistical analyses, we excluded colonies that we were unable to assign to lineage (*n* = 15). To test whether lineages were nonrandomly distributed across the island and across the human disturbance gradient before the heatwave, we conducted a Fisher's exact test and a multinomial regression, respectively. We also conducted pairwise Fisher's tests (correcting with Bonferroni method) between each combination of regions to determine which regions differed significantly in lineage relative abundance. For geographic effects, we divided the island into four regions (North Lagoon Face, *n* = 3 sites; Vaskess Bay/South Lagoon Face, *n* = 5 sites; Bay of Wrecks, *n* = 2 sites; and North Shore, *n* = 3 sites; fig. S5), while we treated human disturbance as a continuous predictor of lineage. We also tested whether algal symbiont communities differed across lineages before the heatwave, using a PERMANOVA on the MED sequence matrix output from SymPortal and on the *Cladocopium* ASV matrix generated from dada2. We visualized MED sequence ordinations (Fig. 3, A and B) using only sequence

reads from the *Cladocopium* C15 clade but included all *Cladocopium* variants in our ordinations on ASV data. We tested for effects of coral lineage and human disturbance on total survival, by conducting a binomial logistic regression with these two variables and an interaction term between them. We performed a similar test with tissue loss as a response using a quasibinomial logistic regression given that these data were proportions. Using the colonies that were assigned to a lineage and tracked through the heatwave (*n* = 78), we tested whether colony size differed between lineages using an ANOVA. We also tested whether there was an effect of size or a size-by-lineage interaction with respect to both total mortality and tissue death using GLMs (binomial and quasibinomial, respectively). We tested for differences in categorical bleaching status across lineages both early and late in the heatwave using ordinal logistic regressions. These analyses were run primarily using the following packages in R: ape (*112*), bayesfactor (*113*), dada2 (*98*), paco (*102*), phyloseq (*99*), tidyverse (*114*), vegan (*115*), and vgam (*116*).

Supplementary Materials

This PDF file includes:
Figs. S1 to S23
Tables S1 to S9
Legends for files S1 and S2

Other Supplementary Material for this manuscript includes the following:
Files S1 and S2

REFERENCES AND NOTES

1. A. Rammig, M. D. Mahecha, Ecosystem responses to climate extremes. *Nature* **527**, 315–316 (2015).
2. M. D. Smith, The ecological role of climate extremes: Current understanding and future prospects. *J. Ecol.* **99**, 651–655 (2011).
3. S. Legg, Climate change 2021—The physical science basis. *Int. Panel Clim. Change* **49**, 44–45 (2021).
4. T. Wernberg, S. Bennett, R. C. Babcock, T. de Bettignies, K. Cure, M. Depczynski, F. Dufois, J. Fromont, C. J. Fulton, R. K. Hovey, E. S. Harvey, T. H. Holmes, G. A. Kendrick, B. Radford, J. Santana-Garcon, B. J. Saunders, D. A. Smale, M. S. Thomsen, C. A. Tuckett, F. Tuya, M. A. Vanderklift, S. Wilson, Climate-driven regime shift of a temperate marine ecosystem. *Science* **353**, 169–172 (2016).
5. D. A. Smale, T. Wernberg, E. C. J. Oliver, M. Thomsen, B. P. Harvey, S. C. Straub, M. T. Burrows, L. V. Alexander, J. A. Benthuysen, M. G. Donat, M. Feng, A. J. Hobday, N. J. Holbrook, S. E. Perkins-Kirkpatrick, H. A. Scannell, A. S. Gupta, B. L. Payne, P. J. Moore, Marine heatwaves threaten global biodiversity and the provision of ecosystem services. *Nat. Clim. Change* **9**, 306–312 (2019).
6. E. I. A. y Juárez, E. A. Ellis, E. Rodríguez-Luna, Quantifying the severity of hurricanes on extinction probabilities of a primate population: Insights into "Island" extirpations. *Am. J. Primatol.* **77**, 786–800 (2015).
7. M. Romero-Torres, A. Acosta, A. M. Palacio-Castro, E. A. Treml, F. A. Zapata, D. A. Paz-García, J. W. Porter, Coral reef resilience to thermal stress in the Eastern Tropical Pacific. *Glob. Chang. Biol.* **26**, 3880–3890 (2020).
8. H. Tanaka, M. Yasuhara, J. T. Carlton, Transoceanic transport of living marine Ostracoda (Crustacea) on tsunami debris from the 2011 Great East Japan Earthquake. *Aquatic Invasions* **13**, 125–135 (2018).
9. P. R. Grant, B. R. Grant, R. B. Huey, M. T. J. Johnson, A. H. Knoll, J. Schmitt, Evolution caused by extreme events. *Philos. Trans. R. Soc. B Biol. Sci.* **372**, 20160146 (2017).
10. M. A. Coleman, T. Wernberg, The silver lining of extreme events. *Trends Ecol. Evol.* **35**, 1065–1067 (2020).
11. T. C. LaJeunesse, R. Smith, M. Walther, J. Pinzón, D. T. Pettay, M. McGinley, M. Aschaffenburg, P. Medina-Rosas, A. L. Cupul-Magaña, A. L. Pérez, H. Reyes-Bonilla, M. E. Warner, Host–symbiont recombination versus natural selection in the response of

coral–dinoflagellate symbioses to environmental disturbance. *Proc. Biol. Sci.* **277**, 2925–2934 (2010).

12. C. Gurgel, O. Camacho, A. Minne, T. Wernberg, M. Coleman, Marine heatwave drives cryptic loss of genetic diversity in underwater forests. *Curr. Biol.* **30**, 1199–1206.e2 (2020).

13. A. G. Little, D. N. Fisher, T. W. Schoener, J. N. Pruitt, Population differences in aggression are shaped by tropical cyclone-induced selection. *Nat. Ecol. Evol.* **3**, 1294–1297 (2019).

14. S. C. Campbell-Staton, Z. A. Cheviron, N. Rochette, J. Catchen, J. B. Losos, S. V. Edwards, Winter storms drive rapid phenotypic, regulatory, and genomic shifts in the green anole lizard. *Science* **357**, 495–498 (2017).

15. D. Lirman, S. Schopmeyer, D. Manzello, L. J. Gramer, W. F. Precht, F. Muller-Karger, K. Banks, B. Barnes, E. Bartels, A. Bourque, J. Byrne, S. Donahue, J. Duquesnel, L. Fisher, D. Gilliam, J. Hendee, M. Johnson, K. Maxwell, E. McDevitt, J. Monty, D. Rueda, R. Ruzicka, S. Thanner, Severe 2010 cold-water event caused unprecedented mortality to corals of the florida reef tract and reversed previous survivorship patterns. *PLOS ONE* **6**, e23047 (2011).

16. J. A. Harvey, M. P. Thakur, J. Ellers, The tarnished silver lining of extreme climatic events. *Trends Ecol. Evol.* **36**, 384–385 (2021).

17. S. U. Pauls, C. Nowak, M. Bálint, M. Pfenninger, The impact of global climate change on genetic diversity within populations and species. *Mol. Ecol.* **22**, 925–946 (2013).

18. T. P. Hughes, K. D. Anderson, S. R. Connolly, S. F. Heron, J. T. Kerry, J. M. Lough, A. H. Baird, J. K. Baum, M. L. Berumen, T. C. Bridge, D. C. Claar, C. M. Eakin, J. P. Gilmour, N. A. J. Graham, H. Harrison, J.-P. A. Hobbs, A. S. Hoey, M. Hoogenboom, R. J. Lowe, M. T. McCulloch, J. M. Pandolfi, M. Pratchett, V. Schoepf, G. Torda, S. K. Wilson, Spatial and temporal patterns of mass bleaching of corals in the Anthropocene. *Science* **359**, 80–83 (2018).

19. A. J. Hobday, L. V. Alexander, S. E. Perkins, D. A. Smale, S. C. Straub, E. C. Oliver, J. A. Benthuysen, M. T. Burrows, M. G. Donat, M. Feng, A hierarchical approach to defining marine heatwaves. *Progress Oceanogr.* **141**, 227–238 (2016).

20. T. L. Frölicher, E. M. Fischer, N. Gruber, Marine heatwaves under global warming. *Nature* **560**, 360–364 (2018).

21. J. M. T. Magel, S. A. Dimoff, J. K. Baum, Direct and indirect effects of climate change–amplified pulse heat stress events on coral reef fish communities. *Ecol. Appl.* **30**, e02124 (2020).

22. M. A. Coleman, A. J. P. Minne, S. Vranken, T. Wernberg, Genetic tropicalisation following a marine heatwave. *Sci. Rep.* **10**, 12726 (2020).

23. S. C. Burgess, E. C. Johnston, A. S. Wyatt, J. J. Leichter, P. J. Edmunds, Response diversity in corals: Hidden differences in bleaching mortality among cryptic *Pocillopora* species. *Ecology* **102**, e03324 (2021).

24. S. P. Brady, D. I. Bolnick, A. L. Angert, A. Gonzalez, R. D. H. Barrett, E. Crispo, A. M. Derry, C. G. Eckert, D. J. Fraser, G. F. Fussmann, F. Guichard, T. Lamy, A. G. McAdam, A. E. M. Newman, A. Paccard, G. Rolshausen, A. M. Simons, A. P. Hendry, Causes of mal-adaptation. *Evol. Appl.* **12**, 1229–1242 (2019).

25. N. H. Barton, The role of hybridization in evolution. *Mol. Ecol.* **10**, 551–568 (2001).

26. A. Suarez-Gonzalez, C. Lexer, Q. C. B. Cronk, Adaptive introgression: A plant perspective. *Biol. Lett.* **14**, 20170688 (2018).

27. J. T. Ladner, S. R. Palumbi, Extensive sympatry, cryptic diversity and introgression throughout the geographic distribution of two coral species complexes. *Mol. Ecol.* **21**, 2224–2238 (2012).

28. Z. H. Forsman, D. J. Barshis, C. L. Hunter, R. J. Toonen, Shape-shifting corals: Molecular markers show morphology is evolutionarily plastic in Porites. *BMC Evol. Biol.* **9**, 45 (2009).

29. Z. H. Forsman, R. Ritson-Williams, K. H. Tisthammer, I. S. S. Knapp, R. J. Toonen, Host-symbiont coevolution, cryptic structure, and bleaching susceptibility, in a coral species complex (Scleractinia; Poritidae). *Sci. Rep.* **10**, 1–12 (2020).

30. J. E. Fifer, N. Yasuda, T. Yamakita, C. B. Bove, S. W. Davies, Genetic divergence and range expansion in a western North Pacific coral. *Sci. Total Environ.* **813**, 152423 (2022).

31. R. W. Buddemeier, D. G. Fautin, Coral bleaching as an adaptive mechanism. *Bioscience* **43**, 320–326 (1993).

32. T. C. LaJeunesse, J. E. Parkinson, P. W. Gabrielson, H. J. Jeong, J. D. Reimer, C. R. Voolstra, S. R. Santos, Systematic revision of Symbiodiniaceae highlights the antiquity and diversity of coral endosymbionts. *Curr. Biol.* **28**, 2570–2580.e6 (2018).

33. P. W. Glynn, Coral reef bleaching: Facts, hypotheses and implications. *Glob. Chang. Biol.* **2**, 495–509 (1996).

34. J. P. G. Spurgeon, The economic valuation of coral reefs. *Mar. Pollut. Bull.* **24**, 529–536 (1992).

35. S. V. Vollmer, S. R. Palumbi, Hybridization and the evolution of reef coral diversity. *Science* **296**, 2023–2025 (2002).

36. K. R. Hind, S. Starko, J. M. Burt, M. A. Lemay, A. K. Salomon, P. T. Martone, Trophic control of cryptic coralline algal diversity. *Proc. Natl. Acad. Sci. U.S.A.* **116**, 15080–15085 (2019).

37. M. J. Brasier, H. Wiklund, L. Neal, R. Jeffreys, K. Linse, H. Ruhl, A. G. Glover, DNA barcoding uncovers cryptic diversity in 50% of deep-sea Antarctic polychaetes. *R. Soc. Open Sci.* **3**, 160432 (2016).

38. E. Anderson, Introgressive hybridization, in *Introgressive Hybridization* (John Wiley and Sons, 1949).

39. N. H. Rose, R. A. Bay, M. K. Morikawa, L. Thomas, E. A. Sheets, S. R. Palumbi, Genomic analysis of distinct bleaching tolerances among cryptic coral species. *Proc. R. Soc. B Biol. Sci.* **288**, 20210678 (2021).

40. M. Gómez-Corrales, C. Prada, Cryptic lineages respond differently to coral bleaching. *Mol. Ecol.* **29**, 4265–4273 (2020).

41. D. C. Claar, S. Starko, K. L. Tietjen, H. E. Epstein, R. Cunning, K. M. Cobb, A. C. Baker, R. D. Gates, J. K. Baum, Dynamic symbioses reveal pathways to coral survival through prolonged heatwaves. *Nat. Commun.* **11**, 6097 (2020).

42. E. C. Johnston, R. Cunning, S. C. Burgess, Cophylogeny and specificity between cryptic coral species (Pocillopora spp.) at Mo'orea and their symbionts (Symbiodiniaceae). *Mol. Ecol.* **31**, 5368–5385 (2022).

43. N. H. Rose, R. A. Bay, M. K. Morikawa, S. R. Palumbi, Polygenic evolution drives species divergence and climate adaptation in corals. *Evolution* **72**, 82–94 (2018).

44. C. Prada, M. E. Hellberg, Long prereproductive selection and divergence by depth in a Caribbean candelabrum coral. *Proc. Natl. Acad. Sci. U.S.A.* **110**, 3961–3966 (2013).

45. M. J. van Oppen, P. Bongaerts, P. Frade, L. M. Peplow, S. E. Boyd, H. T. Nim, L. K. Bay, Adaptation to reef habitats through selection on the coral animal and its associated microbiome. *Mol. Ecol.* **27**, 2956–2971 (2018).

46. C. M. Eakin, H. P. Sweatman, R. E. Brainard, The 2014–2017 global-scale coral bleaching event: Insights and impacts. *Coral Reefs* **38**, 539–545 (2019).

47. T. P. Hughes, J. T. Kerry, M. Álvarez-Noriega, J. G. Álvarez-Romero, K. D. Anderson, A. H. Baird, R. C. Babcock, M. Beger, D. R. Bellwood, R. Berkelmans, Global warming and recurrent mass bleaching of corals. *Nature* **543**, 373–377 (2017).

48. T. D. Ainsworth, S. F. Heron, J. C. Ortiz, P. J. Mumby, A. Grech, D. Ogawa, C. M. Eakin, W. Leggat, Climate change disables coral bleaching protection on the Great Barrier Reef. *Science* **352**, 338–342 (2016).

49. J. K. Baum, D. C. Claar, K. L. Tietjen, J. M. Magel, D. G. Maucieri, K. M. Cobb, J. M. McDevitt-Irwin, Transformation of coral communities subjected to an unprecedented heatwave is modulated by local disturbance. *Sci. Adv.* **9**, eabq5615 (2023).

50. T. I. Terraneo, F. Benzoni, R. Arrigoni, A. H. Baird, K. G. Mariappan, Z. H. Forsman, M. K. Wooster, J. Bouwmeester, A. Marshell, M. L. Berumen, Phylogenomics of *Porites* from the Arabian Peninsula. *Mol. Phylogenet. Evol.* **161**, 107173 (2021).

51. X. Liu, Y.-X. Fu, Exploring population size changes using SNP frequency spectra. *Nat. Genet.* **47**, 555–559 (2015).

52. J. Jouganous, W. Long, A. P. Ragsdale, S. Gravel, Inferring the joint demographic history of multiple populations: Beyond the diffusion approximation. *Genetics* **206**, 1549–1567 (2017).

53. M. T. Connelly, C. J. McRae, P.-J. Liu, N. Traylor-Knowles, Lipopolysaccharide treatment stimulates Pocillopora coral genotype-specific immune responses but does not alter coral-associated bacteria communities. *Dev. Comp. Immunol.* **109**, 103717 (2020).

54. B. C. Hume, E. G. Smith, M. Ziegler, H. J. Warrington, J. A. Burt, T. C. LaJeunesse, J. Wiedenmann, C. R. Voolstra, SymPortal: A novel analytical framework and platform for coral algal symbiont next-generation sequencing ITS2 profiling. *Mol. Ecol. Resour.* **19**, 1063–1080 (2019).

55. K. M. Quigley, B. Ramsby, P. Laffy, J. Harris, V. J. L. Mocellin, L. K. Bay, Symbioses are restructured by repeated mass coral bleaching. *Sci. Adv.* **8**, eabq8349 (2022).

56. R. Cunning, R. N. Silverstein, A. C. Baker, Investigating the causes and consequences of symbiont shuffling in a multi-partner reef coral symbiosis under environmental change. *Proc. R. Soc. B Biol. Sci.* **282**, 20141725 (2015).

57. A. C. Baker, Flexibility and specificity in coral-algal symbiosis: Diversity, ecology, and biogeography of *Symbiodinium*. *Annu. Rev. Ecol. Evol. Syst.* **34**, 661–689 (2003).

58. C. Arif, C. Daniels, T. Bayer, E. Banguera-Hinestroza, A. Barbrook, C. J. Howe, T. C. LaJeunesse, C. R. Voolstra, Assessing symbiodinium diversity in scleractinian corals via next-generation sequencing-based genotyping of the ITS2 rDNA region. *Mol. Ecol.* **23**, 4418–4433 (2014).

59. J. E. Fifer, V. Bui, J. T. Berg, N. Kriefall, C. Klepac, B. Bentlage, S. W. Davies, Microbiome structuring within a coral colony and along a sedimentation gradient. *Science* **8**, 805202 (2022).

60. N. S. Fabina, H. M. Putnam, E. C. Franklin, M. Stat, R. D. Gates, Symbiotic specificity, association patterns, and function determine community responses to global changes: Defining critical research areas for coral-Symbiodinium symbioses. *Glob. Chang. Biol.* **19**, 3306–3316 (2013).

61. S. A. Fay, M. X. Weber, The occurrence of mixed infections of symbiodinium (Dinoflagellata) within individual hosts. *J. Phycol.* **48**, 1306–1316 (2012).

62. Y. T. R. Tan, B. J. Wainwright, S. Afiq-Rosli, Y. C. A. Ip, J. N. Lee, N. T. H. Nguyen, S. B. Pointing, D. Huang, Endosymbiont diversity and community structure in Porites lutea from

Southeast Asia are driven by a suite of environmental variables. *Symbiosis* **80**, 269–277 (2020).

63. A. C. Baker, T. R. McClanahan, C. J. Starger, R. K. Boonstra, Long-term monitoring of algal symbiont communities in corals reveals stability is taxon dependent and driven by site-specific thermal regime. *Mar. Ecol. Prog. Ser.* **479**, 85–97 (2013).

64. A. C. Baker, C. J. Starger, T. R. McClanahan, P. W. Glynn, Corals' adaptive response to climate change. *Nature* **430**, 741–741 (2004).

65. K. M. Quigley, P. A. Warner, L. K. Bay, B. L. Willis, Unexpected mixed-mode transmission and moderate genetic regulation of Symbiodinium communities in a brooding coral. *Heredity* **121**, 524–536 (2018).

66. K. M. Quigley, B. L. Willis, C. D. Kenkel, Transgenerational inheritance of shuffled symbiont communities in the coral Montipora digitata. *Sci. Rep.* **9**, 13328 (2019).

67. M. J. H. van Oppen, J. K. Oliver, H. M. Putnam, R. D. Gates, Building coral reef resilience through assisted evolution. *Proc. Natl. Acad. Sci. U.S.A.* **112**, 2307–2313 (2015).

68. A. H. Moeller, A. Caro-Quintero, D. Mjungu, A. V. Georgiev, E. V. Lonsdorf, M. N. Muller, A. E. Pusey, M. Peeters, B. H. Hahn, H. Ochman, Cospeciation of gut microbiota with hominids. *Science* **353**, 380–382 (2016).

69. A. H. Moeller, T. A. Suzuki, M. Phifer-Rixey, M. W. Nachman, Transmission modes of the mammalian gut microbiota. *Science* **362**, 453–457 (2018).

70. A. Hayward, R. Poulin, S. Nakagawa, A broadscale analysis of host-symbiont cophylogeny reveals the drivers of phylogenetic congruence. *Ecol. Lett.* **24**, 1681–1696 (2021).

71. M. Stat, R. D. Gates, Clade D *Symbiodinium* in scleractinian corals: A "nugget" of hope, a selfish opportunist, an ominous Sign, or all of the above? *J. Mar. Biol.* **2011**, e730715 (2011).

72. K. D. Hoadley, D. T. Pettay, A. Lewis, D. Wham, C. Grasso, R. Smith, D. W. Kemp, T. LaJeunesse, M. E. Warner, Different functional traits among closely related algal symbionts dictate stress endurance for vital Indo-Pacific reef-building corals. *Glob. Chang. Biol.* **27**, 5295–5309 (2021).

73. E. J. Howells, V. H. Beltran, N. W. Larsen, L. K. Bay, B. L. Willis, M. J. H. van Oppen, Coral thermal tolerance shaped by local adaptation of photosymbionts. *Nat. Clim. Change* **2**, 116–120 (2012).

74. D. Bickford, D. J. Lohman, N. S. Sodhi, P. K. L. Ng, R. Meier, K. Winker, K. K. Ingram, I. Das, Cryptic species as a window on diversity and conservation. *Trends Ecol. Evol.* **22**, 148–155 (2007).

75. L. Rüber, J. L. Van Tassell, R. Zardoya, S. Karl, Rapid speciation and ecological divergence in the american seven-spined gobies (gobiidae, Gobiosomatini) inferred from a molecular phylogeny. *Evolution* **57**, 1584–1598 (2003).

76. D. Schluter, Ecological causes of adaptive radiation. *Am. Nat.* **148**, S40–S64 (1996).

77. S. Starko, K. Demes, C. Neufeld, P. Martone, Convergent evolution of niche structure in Northeast Pacific kelp forests. *Funct. Ecol.* **34**, 2131–2146 (2020).

78. D. Ackerly, Conservatism and diversification of plant functional traits: Evolutionary rates versus phylogenetic signal. *Proc. Natl. Acad. Sci. U.S.A.* **106**, 19699–19706 (2009).

79. A. M. Palacio-Castro, T. B. Smith, V. Brandtneris, G. A. Snyder, R. van Hooidonk, J. L. Maté, D. Manzello, P. W. Glynn, P. Fong, A. C. Baker, Increased dominance of heat-tolerant symbionts creates resilient coral reefs in near-term ocean warming. *Proc. Natl. Acad. Sci. U.S.A.* **120**, e2202388120 (2023).

80. D. M. Becker, H. M. Putnam, D. E. Burkepile, T. C. Adam, R. Vega Thurber, N. J. Silbiger, Chronic low-level nutrient enrichment benefits coral thermal performance in a fore reef habitat. *Coral Reefs* **40**, 1637–1655 (2021).

81. M. S. Naugle, T. A. Oliver, D. J. Barshis, R. D. Gates, C. A. Logan, Variation in coral thermotolerance across a pollution gradient erodes as coral symbionts shift to more heat-tolerant genera. *Front. Mar. Sci.* **8**, 760891 (2021).

82. M. J. H. van Oppen, R. D. Gates, L. L. Blackall, N. Cantin, L. J. Chakravarti, W. Y. Chan, C. Cormick, A. Crean, K. Damjanovic, H. Epstein, P. L. Harrison, T. A. Jones, M. Miller, R. J. Pears, L. M. Peplow, D. A. Raftos, B. Schaffelke, K. Stewart, S. Torda, D. Wachenfeld, A. R. Weeks, H. M. Putnam, Shifting paradigms in restoration of the world's coral reefs. *Glob. Chang. Biol.* **23**, 3437–3448 (2017).

83. Q. Cong, J. Shen, D. Borek, R. K. Robbins, P. A. Opler, Z. Otwinowski, N. V. Grishin, When COI barcodes deceive: Complete genomes reveal introgression in hairstreaks. *Proc. Royal Soc. B Biol. Sci.* **284**, 20161735 (2017).

84. R. van Velzen, E. Weitschek, G. Felici, F. T. Bakker, DNA barcoding of recently diverged species: Relative performance of matching methods. *PLOS ONE* **7**, e30490 (2012).

85. N. N. Winchester, R. A. Ring, Centinelan extinctions: Extirpation of northern temperate old-growth rainforest arthropod communities. *Selbyana* **17**, 50–57 (1996).

86. O. Morate, *Population and Housing Census Volume 1: Management Report and Basic Tables* (National Statistics Office, Ministry of Finance, Bairiki, Tarawa, Republic of Kiribati, 2015).

87. M. S. Watson, D. C. Claar, J. K. Baum, Subsistence in isolation: Fishing dependence and perceptions of change on Kiritimati, the world's largest atoll. *Ocean Coastal Manag.* **123**, 1–8 (2016).

88. T. R. McClanahan, E. S. Darling, J. M. Maina, N. A. Muthiga, S. D. 'agata, S. D. Jupiter, R. Arthur, S. K. Wilson, S. Mangubhai, Y. Nand, A. M. Ussi, A. T. Humphries, V. J. Patankar, M. M. M. Guillaume, S. A. Keith, P. Shedrawi, G. Julius, G. Grimsditch, J. Ndagala, J. Leblond, Temperature patterns and mechanisms influencing coral bleaching during the 2016 El Niño. *Nat. Clim. Chang.* **9**, 845–851 (2019).

89. M. Stat, W. K. W. Loh, T. C. LaJeunesse, O. Hoegh-Guldberg, D. A. Carter, Stability of coral–Endosymbiont associations during and after a thermal stress event in the southern Great Barrier Reef. *Coral Reefs* **28**, 709–713 (2009).

90. I. B. Baums, C. R. Hughes, M. E. Hellberg, Mendelian microsatellite loci for the Caribbean coral Acropora palmata. *Mar. Ecol. Prog. Ser.* **288**, 115–127 (2005).

91. S. Wang, E. Meyer, J. K. McKay, M. V. Matz, 2b-RAD: A simple and flexible method for genome-wide genotyping. *Nat. Methods* **9**, 808–810 (2012).

92. M. Aranda, Y. Li, Y. J. Liew, S. Baumgarten, O. Simakov, M. C. Wilson, J. Piel, H. Ashoor, S. Bougouffa, V. B. Bajic, T. Ryu, T. Ravasi, T. Bayer, G. Micklem, H. Kim, J. Bhak, T. C. LaJeunesse, C. R. Voolstra, Genomes of coral dinoflagellate symbionts highlight evolutionary adaptations conducive to a symbiotic lifestyle. *Sci. Rep.* **6**, 39734 (2016).

93. H. Liu, T. G. Stephens, R. A. González-Pech, V. H. Beltran, B. Lapeyre, P. Bongaerts, I. Cooke, M. Aranda, D. G. Bourne, S. Forêt, D. J. Miller, M. J. H. van Oppen, C. R. Voolstra, M. A. Ragan, C. X. Chan, Symbiodinium genomes reveal adaptive evolution of functions related to coral-dinoflagellate symbiosis. *Commun. Biol.* **1**, 1–11 (2018).

94. E. Shoguchi, C. Shinzato, T. Kawashima, F. Gyoja, S. Mungpakdee, R. Koyanagi, T. Takeuchi, K. Hisata, M. Tanaka, M. Fujiwara, M. Hamada, A. Seidi, M. Fujie, T. Usami, H. Goto, S. Yamasaki, N. Arakaki, Y. Suzuki, S. Sugano, A. Toyoda, Y. Kuroki, A. Fujiyama, M. Medina, M. A. Coffroth, D. Bhattacharya, N. Satoh, Draft assembly of the symbiodinium minutum nuclear genome reveals dinoflagellate gene structure. *Curr. Biol.* **23**, 1399–1408 (2013).

95. B. Langmead, S. L. Salzberg, Fast gapped-read alignment with Bowtie 2. *Nat. Methods* **9**, 357–359 (2012).

96. Y. J. Liew, M. Aranda, C. R. Voolstra, Reefgenomics.Org—A repository for marine genomics data. *Database* **2016**, baw152 (2016).

97. T. S. Korneliussen, A. Albrechtsen, R. Nielsen, ANGSD: Analysis of next generation sequencing data. *BMC Bioinformatics* **15**, 1–13 (2014).

98. B. J. Callahan, P. J. McMurdie, M. J. Rosen, A. W. Han, A. J. A. Johnson, S. P. Holmes, DADA2: High-resolution sample inference from Illumina amplicon data. *Nat. Methods* **13**, 581–583 (2016).

99. P. J. McMurdie, S. Holmes, phyloseq: An R package for reproducible interactive analysis and graphics of microbiome census data. *PLOS ONE* **8**, e61217 (2013).

100. M. Kearse, R. Moir, A. Wilson, S. Stones-Havas, M. Cheung, S. Sturrock, S. Buxton, A. Cooper, S. Markowitz, C. Duran, Geneious Basic: An integrated and extendable desktop software platform for the organization and analysis of sequence data. *Bioinformatics* **28**, 1647–1649 (2012).

101. D. H. Alexander, S. S. Shringarpure, J. Novembre, K. Lange, *Admixture 1.3 Software Manual* (UCLA Human Genetics Software Distribution, 2015).

102. M. C. Hutchinson, E. F. Cagua, J. A. Balbuena, D. B. Stouffer, T. Poisot, paco: Implementing procrustean approach to cophylogeny in R. *Methods Ecol. Evol.* **8**, 932–940 (2017).

103. A. Stamatakis, RAxML version 8: A tool for phylogenetic analysis and post-analysis of large phylogenies. *Bioinformatics* **30**, 1312–1313 (2014).

104. M. Foll, BayeScan v2. 1 user manual. *Ecology* **20**, 1450–1462 (2012).

105. J. P. Rippe, G. Dixon, Z. L. Fuller, Y. Liao, M. Matz, Environmental specialization and cryptic genetic divergence in two massive coral species from the florida keys reef tract. *Mol. Ecol.* **30**, 3468–3484 (2021).

106. X. Liu, Y.-X. Fu, Stairway Plot 2: Demographic history inference with folded SNP frequency spectra. *Genome Biol.* **21**, 280 (2020).

107. C. Prada, M. B. DeBiasse, J. E. Neigel, B. Yednock, J. L. Stake, Z. H. Forsman, I. B. Baums, M. E. Hellberg, Genetic species delineation among branching Caribbean Porites corals. *Coral Reefs* **33**, 1019–1030 (2014).

108. V. J. Harriott, Reproductive ecology of four scleratinian species at Lizard Island, Great Barrier Reef. *Coral Reefs* **2**, 9–18 (1983).

109. J. Pätzold, Growth rhythms recorded in stable isotopes and density bands in the reef coral Porites lobata (Cebu, Philippines). *Coral Reefs* **3**, 87–90 (1984).

110. K. Luu, E. Bazin, M. G. B. Blum, pcadapt: An R package to perform genome scans for selection based on principal component analysis. *Mol. Ecol. Resour.* **17**, 67–77 (2017).

111. H. Rivera, A. Cohen, J. Thompson, I. Baums, M. Fox, K. Meyer, Palau's warmest reefs harbor a thermally tolerant coral lineage that thrives across different habitats. *Commun. Biol.* **5**, 1394 (2022).

112. E. Paradis, K. Schliep, ape 5.0: An environment for modern phylogenetics and evolutionary analyses in R. *Bioinformatics* **35**, 526–528 (2019).

113. R. D. Morey, J. N. Rouder, T. Jamil, M. R. D. Morey, Package 'bayesfactor' (2015); https://cran.r-project.org/web/packages/BayesFactor/index.html.

114. H. Wickham, M. Averick, J. Bryan, W. Chang, L. McGowan, R. François, G. Grolemund, A. Hayes, L. Henry, J. Hester, Welcome to the tidyverse. *J. Open Source Softw.* **4**, 1686 (2019).

115. J. Oksanen, F. G. Blanchet, R. Kindt, P. Legendre, R. B. O'hara, G. L. Simpson, P. Solymos, M. H. H. Stevens, H. Wagner, Vegan: Community ecology package. R package version 1.17-4 (2010); http://cran.r-project.org.

116. T. W. Yee, The VGAM package for categorical data analysis. *J. Stat. Softw.* **32**, 1–34 (2010).

Science Advances

Marine heatwaves threaten cryptic coral diversity and erode associations among coevolving partner

Samuel Starko, James E. Fifer, Danielle C. Claar, Sarah W. Davies, Ross Cunning, Andrew C. Baker, and Julia K. Baum

View the article online
https://www.science.org/doi/10.1126/sciadv.adf0954
Permissions
https://www.science.org/help/reprints-and-permissions

Use of this article is subject to the Terms of service